LITHIATION OF METAL-OXIDE THIN FILM LAYERS ON ZTO/AG/ZTO ELECTRODES BY MAGNETRON SPUTTERING FOR ELECTROCHROMIC DEVICES

A Thesis Submitted to
The Graduate School of Engineering and Sciences of
Izmir Institute of Technology
in Partial Fulfilment of the Requirements for the Degree of
MASTER OF SCIENCE

in Energy Systems Engineering

by
Enver DEVECİ

July 2023

İZMİR

We approve the thesis of **Enver DEVECİ**

Examining Committee Members:

_____

Prof. Dr. Lütfi ÖZYÜZER
Head of the Department of Physics,
Izmir Institute of Technology

_____

Prof. Dr. Emre GÜR
Department of Physics, Eskisehir Osmangazi University

_____

Doç. Dr. Enver TARHAN
Department of Physics, Izmir Institute of Technology

11 July 2023

_____

Prof. Dr. Lütfi ÖZYÜZER
Supervisor, Head of the Department of Physics,
Izmir Institute of Technology

_____

Assoc. Prof. Dr. Uğur ÜNAL
Co-advisor, Department of
Chemistry, Koc University

_____

Prof. Dr. Gülden GÖKÇEN AKKURT
Head of the Energy Systems Engineering,
Izmir Institute of Technology

_____

Prof. Dr. Mehtap EANES
Dean of the Graduate School of
Engineering and Sciences,
Izmir Institute of Technology

ACKNOWLEDGEMENTS

I would like to express the deepest appreciation to my committee chair, Prof. Dr. Lütfi ÖZYÜZER for his valuable advice, comprehensive and morally supports he gave me and Doç. Dr. Uğur ÜNAL for his valuable contribution and guidance throughout the research process. I also would like to acknowledge that this project is partially supported by TEKNOMA Technological Materials Inc. Furthermore, I would like to thank Dr. Mehtap ÖZDEMİR for her excellent guidance, continuous support, and understanding throughout my thesis. Her deep insights helped me at various stages of my research.

I would like to thank the rest members of my thesis defence committee Prof. Dr. Emre GÜR and Doç Dr. Enver TARHAN for giving suggestions and helpful comments. I am also very thankful to my colleagues from Izmir Institute of Technology and my fellow labmates in OZYUZER Research Group members.

Also, I would like to thank my mother Havva and father Şaban, who were always there for me and did not spare their support and love. I would like to thank my sister Çiğdem Nur, who always thinks of me going forward more than I do. I've always felt lucky to be in this family.

This work was supported by TUBITAK - TEYDEB project number 3192182.

ABSTRACT

LITHIATION OF METAL-OXIDE THIN FILM LAYERS ON ZTO/AG/ZTO ELECTRODES BY MAGNETRON SPUTTERING FOR ELECTROCHROMIC DEVICES

Electrochromism is a property of materials that undergoes a reversible transition from a colorless or transparent state to a colored state under the action of electric voltage or current. What makes electrochromic materials special is by controlling the voltage applied to the material. Among these electrochromic materials, metal oxides such as WO_3 and NiO_x are metal oxides that are frequently used. Electrochromic devices are devices that do not consume much energy and can save a lot of energy. A typical electrochromic device consists of five different thin film layers: an ionic conductive layer (electrolyte) and the transparent conductive oxides (ITO, FTO, ZTO etc.) cover electrochromic layers.

In this study, instead of the traditionally used transparent conductive electrode ITO, ZTO/Ag/ZTO ($Z=Zn_2SnO_4$, ZAZ) electrode with high optical transmittance and electrical conductivity was used, thus cost-effective and more efficient electrochromic devices were produced. Here, 3 layers of thin film (WO_3, Ta_2O_5, NiO_x) coating on glass/ZAZ samples was grown by magnetron sputtering method at room temperature and the production parameters were optimized. WO_3 and NiO_x on ITO (Indium Tin Oxide) were measured, while Ta_2O_5 is used as solid-state electrolyte. Furthermore, WO_3 and NiO_x thin films were lithiated in 1 M $LiClO_4$-PC electrolyte using a conventional three-electrode configuration. In the next step, to test the performance of WO_3 and NiO_x electrochromic device (glass/ZAZ/NiO_x/Ta_2O_5/WO_3/ZAZ) were tested.

ÖZET

ELEKTROKROMİK AYGITLAR İÇİN MIKNATISSAL SAÇTIRMA İLE ZTO/AG/ZTO ELEKTROTLAR ÜZERİNDEKİ METAL-OKSİT İNCE FİLM KATMANLARININ LİTYUMLANMASI

Elektrokromizm, elektrik voltajının veya akımın etkisiyle tersinir bir şekilde, renksiz veya şeffaf bir durumdan renkli bir duruma geçiş gösteren malzemelerin bir özelliğidir. Elektrokromik malzemeleri özel kılan durum, malzemeye uygulanan gerilimi kontrol ederek Bu elektrokromik malzemeler arasında WO_3 ve NiO_x gibi metal oksitler sıkça kullanılan metal oksitlerdir.

Elektrokromik cihazlar fazla enerji harcamayan ve büyük oranda enerji tasarrufu sağlayabilen cihazlardır. Tipik bir elektrokromik cihaz beş farklı ince film katmanından oluşur: iyonik iletken katman (elektrolit) ve şeffaf iletken oksitler (ITO, FTO, ZTO vb.) elektrokromik katmanları kapsar.

Bu çalışmada, geleneksel olarak kullanılan şeffaf iletken elektrot ITO yerine optik geçirgenliği ve elektriksel iletkenliği yüksek ZTO/Ag/ZTO ($Z=Zn_2SnO_4$, ZAZ) elektrot olarak kullanılmış olup, böylece maliyeti uygun ve daha verimli elektrokromik aygıtlar üretilmiştir. Burada cam/ZAZ örneklerinin üzerine 3 kat ince film (WO_3, Ta_2O_5, NiO_x) kaplama mıknatıssal saçtırma yöntemi ile oda sıcaklığında büyütülüp, üretim parametreleri optimize edilmiştir. Burada WO_3 ve NiO_x ince filmleri ITO (Indium Tin Oxide) üstünde büyütülmüştür, Ta_2O_5 ise katı hal elektrolit olarak kullanılmıştır.Ayrıca WO_3 ve NiO_x ince filmleri, gelenekel üç elektrotlu konfigürasyon olarak 1 M $LiClO_4$-PC elektrolit içerisinde lityumlaştırıldı. Bir sonraki adımda WO_3 ve NiO_x elektrokromik filmlerin performansını test etmek için elektrokromik cihaz (cam/ZAZ/NiO_x/Ta_2O_5/WO_3/ZAZ) test edildi.

To my
family…

TABLE OF CONTENTS

LIST OF FIGURES

Figure **Page**

LIST OF TABLES

Table **Page**

CHAPTER 1

INTRODUCTION

1.1. Electrochromism

Chromism is a Greek word meaning color. Chromism refers to the reversible change of optical properties of materials under environmental conditions such as mechanical, electric field, optical, or thermal (Pandurang, 2017). The change in optical properties means a change in the transmittance, reflectance, and absorption properties of the material. Chromic devices depending on the stimulating factor; electrochromic (depending on the applied electric field), photochromic (depending on UV radiation), magneto chromic (depending on the applied magnetic field), etc. can be classified (Bamfield, 2010).

Electrochromism is an optical phenomenon that expresses the reversible color changes observed in the material because of electrochemical reduction (taking electrons) / oxidation (donating electrons) reactions in the material. Materials produced with technology based on this optical phenomenon are called 'electrochromic materials'. The coloration that occurs because of reduction or oxidation events was first called 'electrochromism' by J. R. Platt in 1961(Platt, 1961).

1.2. The History of Electrochromism

The first electrochromic device (EC) was documented by Deb in 1969. Deb has shown that using WO_3 the material causes a controlled and reversible color change (Xu et al., 2019). Since then, devices containing various classifications of electrochromic materials and compatible materials such as metal oxides, violgens, and bonded polymers have been reported. Due to their distinct color changes in the visible region, electrochromic materials have received great

attention and have been used in optical display applications. In the first half of the 1970s, large international companies such as IBM, Zenith Radio, American Cynamid Corporation and RCA in the USA, Canon in Japan, Brown Boveri in Switzerland, and Philips in the Netherlands made extensive studies on electrochromic materials (Xu et al., 2019).

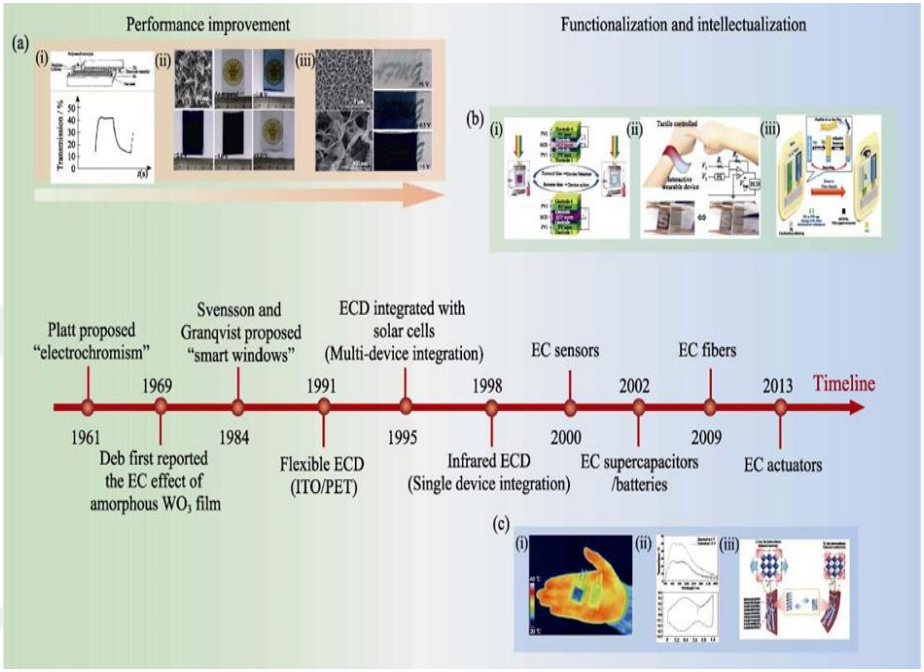

Figure 1.1. Development history of electrochromism: from high performance to intelligence (a) EC electrodes and devices for smart windows: (i) Structure and performance of early ECD, (ii) Self-weaving WO_3 nanoflake EC films, (iii) Nest-like WO_3 EC films; (b) Multi-device integration based on electrochromism: (i) Integration of ECD and photovoltaic cell, (ii) Integration of ECD and tactile sensor, (iii) Integration of ECD and strain sensor; (c) Single device integration based on electrochromism: (i) Electrochromic infrared control, (ii) Electrochromic supercapacitor, (iii) Electrochromic actuator (Source; Hongwei et al., 2021)

1.3. Review of Electrochromic (EC) Devices

Electrochromic devices are devices that reversibly change the optical properties of the material (absorption, transmittance, and reflection) as a result of the application of a certain voltage. Thanks to the transparent conductive oxides used in these devices, they are the materials that enable the metal oxide thin films in the interlayers to occur from bleached to colored and reversibly by using the electrochemical method (Aparicio et al., 2012).

Metal oxides (WO_3, NiO_x, MoO_3, and V_2O_5) have been used as an inorganic EC material where small cations (H^+, Li^+, etc.) enter the crystal lattice and result in color changes through intervalence charge transfer induced by an applied voltage. These metal oxide-based EC devices operate at low voltages with efficient electrical energy consumption and show high optical contrast between colored and bleached states (Baeck et al., 2003; Kongsat et al., 2021).EC devices are commonly utilized as smart windows, information displays, variable-reflectance mirrors, and auto dimming rear-view mirrors in automobiles (Aparicio et al., 2012).

EC-based smart windows contribute to blocking the near-infrared (IR), thereby minimizing heating in airconditioned-based smart green buildings. Depending on the material being used, EC devices can be categorized into inorganic metal oxides, metal complexes, hybrid materials, metal plasmonic–metal/alloy, and organic molecules/conjugated polymers (CPs) (Rai et al., 2012).

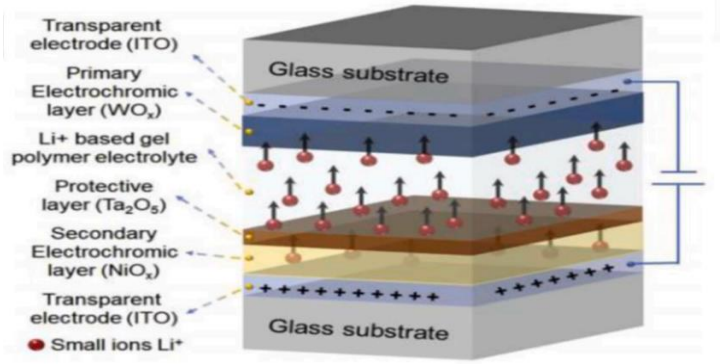

Figure 1.2. $LiClO_4$-PC-PMMA gel-polymer based ECD design (Source; Ding et al.,2022)

1.4. The Purpose of This Thesis

The aim of the study in this thesis is to produce an electrochromic device with an all-inorganic solid-state thin film layer. Liquid/gel electrolyte is used in electrochromic devices available in the market, which causes a problem to flow over time, especially in summer with the effect of hot air. For this reason, solid electrolytes will be used instead of gel, which will eliminate the flow problem. In addition, using indium tin oxide (ITO) as a porous electrode in conventional electrodes increases the cost due to the indium content. Therefore, a cost-effective ZTO(Zinc-Tin-Oxide)/Ag/ZTO electrode with better optical transmittance and electrical conductivity will be used instead of ITO.

With the successful completion of this thesis, the development of ZTO/Ag/ZTO electrode-based electrochromic glass technology (smart glass), the production of very thin devices that save energy and the improvement of today's technologies will be provided. In this way, some general usage areas of glass technology (protection from sunlight, protection from harmful ultraviolet rays, reducing energy loss, privacy and camouflage, architecture, commercial areas, markets, offices, automobiles, and airplanes) will also be developed.

CHAPTER 2

BACKGROUND INFORMATION

2.1. Electrochromic Materials

Electrochromic materials are also defined as 'electrochromes' according to some sources. For example, electrochromes that color in their oxidized state is known as anodic colorants, and those that color in their reduced state is called cathodic coloring electrochromes (Granqvist et al., 2018; Dong et al., 2018).

EC materials have an extraordinary variety of applications, such as self-dimming rear-view mirrors, information displays and electrochromic e-coatings, smart windows for energy-efficient buildings, electrochromic supercapacitors (Wu et al., 2018).

A wide variety of electrochromic materials such as conjugated conductive polymers, viologens and metal oxides show high coloring efficiency. Thin-film metal oxides are leading the way in the studies, as they show wide optical modulation, high coloration efficiency (CE), cyclic stability, and high ion transition and electronic conductivity, providing a relatively short switching time. (Rosseinsky et al., 2015). There are basically two groups of metal oxides for electrochromic applications. As shown in Figure 2.1., the table of elements shows 'cathodic' colorants under ion intercalation and 'anodic' coloring properties under ion extraction (Rosseninsky et al., 2015; Jittiarporn et al., 2017).

In this study, WO_3 thin films as the basic electrochromic film and NiO_x, which acts as a complementary electrochromic film as the ion storage film, were investigated in the electrochromic device structure.

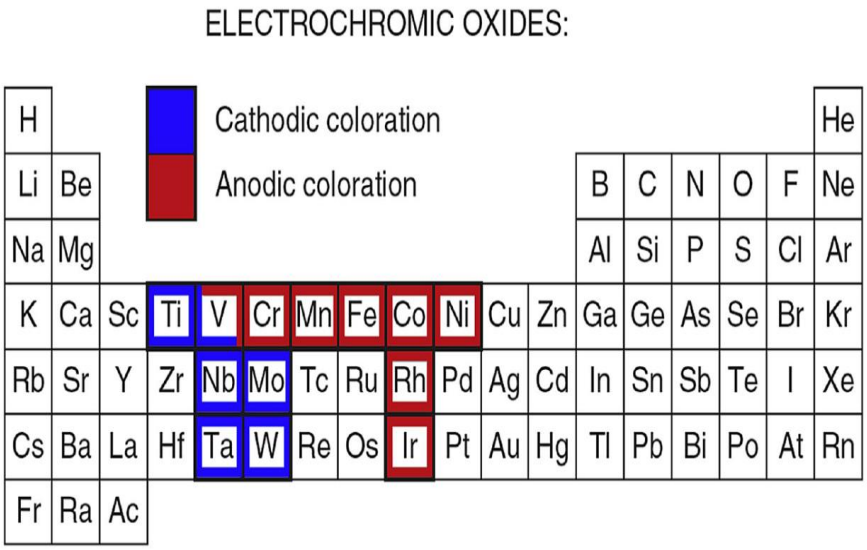

Figure 2.1. Electrochromic transition metal oxides showing both cathodic and anodic coloration. (Source: Rosseninsky et al., 2015; Jittiarporn et al., 2017)

2.2. Tungsten Oxide

WO_3 is one of the transition metals with wide band gap showing n-type semiconductor properties. The crystal structure of this material, which has a density of 7.2 g/cm^3, depends on temperature. It is used in gas and heat sensors, catalysts, electrochromic displays, smart glasses, electrochromic mirrors (Gillaspie et al., 2010; Jiao et al., 2010; Roland et al., 1992). It is one of the most studied cathodic electrochromic materials due to its superior properties such as high coloring efficiency, stability, reversibility, and fast response time (Qiu et al., 2002; Bessière et al., 2002). The growth method and growth parameters of WO_3 thin films determine the electrochromic properties of the film. It can be produced using various magnification methods such as thermal evaporation, magnetron sputtering, sol-gel and pulse laser (Patel et al., 2010; Sauvet et al., 2009; Lin et al., 2009; Ozer et al., 1999).

The coloration mechanism of WO_3 thin films occurs by e^- transfer between W^{+6} and W^{+5}.The general electrochromic phenomenon of WO_3 is due to the formation of tungsten bronze (M_xWO_3). According to the following oxidation-reduction equation:

$$\underset{\text{(Transparent)}}{WO_3} + xe^- + xM^+ = \underset{\text{(Blue)}}{M_xWO_3} \qquad (2.1)$$

where M= Li^+,H^+ or Na^+ etc.

While WO_3 is completely transparent in the oxidized state, it takes on the blue color in the reduced state. The coloration mechanisms are different for amorphous and crystalline WO_3. Electrochromic properties such as cyclic stability and coloration efficiency in WO_3 thin films may vary depending on the morphological, structural properties and composition of the film (Guo et al., 2017; Patel et al., 2010).

Amorphous WO_3 (a-WO_3) is the most popular and most studied electrochromic metal oxide material. It is also used in electrochromic devices whose permeability can be modulated (Wen et al., 2015). WO_3 has led to promising studies in electrochromic windows as its dense crystal structure gives better coloring efficiency and faster response time due to its effect on the ions that will be intercalated through the coloring activity and deintercalated through the bleaching activity (Ding et al., 2018; Zhang et al., 2019).

2.3. Nickel Oxide

Nickel is a very hard, silver-white colored ferromagnetic element. Nickel, which is element 8B, has an atomic number of 28 and an atomic mass of 58.69 g/mol. Its melting point is about 1453 °C, and its boiling point is about 2732 °C. In transition metals, valence electrons are found in more than one shell, so electrons can form compounds with other elements. Nickel is typically divalent

in its oxidized state, exhibiting a +2-oxidation state, but it can also display common oxidation states such as 0, +1, +3, and +4. The electronic configuration of nickel is [Ar] $4s^2 3d^8$. It exhibits magnetic and chemical properties like iron and cobalt. Nickel forms useful alloys with many metals, and its hardness, strength, and corrosion resistance vary depending on the added metal. The most familiar nickel-iron alloys are stainless steel and metal coins (Al-Kahlout et al., 2006). Nickel can also form compounds with elements such as sulphur, oxygen, and chlorine. In electrochromic applications, nickel is used in its oxide state (Abu-Yaqoub et al., 2012). By forming bonds with oxygen, nickel can create different compounds, and these compounds can exist in different phases. In electrochromic applications, the commonly active compounds are Ni $(OH)_2$ and NiOOH, which are aqueous phases. Ni $(OH)_2$ exhibits similar properties to stoichiometric NiO and is transparent, while NiOOH exhibits similar properties to Ni_2O_3 and is colored.

Nickel oxide typically exhibits a non-stoichiometric structure. In non-stoichiometric nickel oxide, the most common defect types are nickel vacancies (Niklasson et al., 2007; Jang et al., 2009). Nickel vacancies create a balancing effect by extracting electrons from two neighbouring Ni^{+2} ions, leading to the formation of Ni^{+3} ions. This phenomenon is illustrated in the following equation:

$$Ni^{+3} - O^{-2} - V_{Ni}{}^{-2} - O^{-2} - Ni^{+3} \qquad (2.2)$$

The notation -2 represents a double negative charge when compared to Ni^{+2}. Due to the creation of vacancies, the Fermi level descends below the valence band. The position of the Fermi level at a certain point in the energy band of Ni oxide makes it conductive and colored. The presence of the Fermi level in the energy band of Ni oxide contributes to its conductivity and gives it a colorful structure. As a result of the formation of vacancies, the Fermi level descends into the lower regions of the energy band, making Ni oxide conductive and providing it with color.

In the structure of nickel oxide, in addition to Ni vacancies, there are also excessive oxygen-containing defects (Lee et al., 1995). This oxygen causes the

Fermi level to be pushed towards the peaks of the valence band, leading to oxidation from Ni^{+2} to Ni^{+3} around the Ni vacancies. Nickel monoxide behaves like a p-type semiconductor because the 2p band of oxygen influences the Fermi level by surrounding the Ni vacancies. The conductivity in the material is explained as a result of the migration of these vacancies.

The electrochromic reaction of NiO_x in Li^+ ion electrolytes is represented by a two-step reaction process. The first irreversible reaction (Equation 2.3) is associated with the activation process in the initial cycling of NiO_x.

$$NiO_x + \alpha\,(Li^+ + e^-) \rightarrow Li\alpha NiO_x \quad (2.3)$$

$$Li\alpha NiO_x\ \gamma\,(Li^+ + e^-) + Li\beta NiO_x \quad (2.4)$$

The second reaction (Equation 2.4) demonstrates the reversible coloring process where ions are intercalated/deintercalated, and it is linked to the charge transfer between Ni^{2+} and Ni^{3+} states. Carefully controlling the proportion of Ni^{2+} and Ni^{3+} ions play a crucial role in enhancing the electrochromism of NiO_x. The electrochromic reaction process in Li^+ ion electrolytes for NiO_x is expressed as a two-step reaction. The first step reaction (Equation 2.3) is associated with the activation process during the initial cycling of NiO_x. The second reaction (Equation 2.4) demonstrates the reversible coloring process that occurs through the intercalation and deintercalation of ions between Ni^{2+} and Ni^{3+} states (Liu et al., 2018). Precise control of the proportion of Ni^{2+} and Ni^{3+} ions is crucial in improving the electrochromism of NiO_x (Qiu et al., 2018).

2.4. Tantalum Pentoxide

Tantalum pentoxide (Ta_2O_5) is frequently used in optical and electronic applications. High visibility, high dielectric constant, high transmittance in the UV region, low leakage current and high chemical and thermal stability have made this material interesting in many fields. It has a high refractive index of 2.18 at 550 nm, low absorption, and wide band gap (~4 eV) (Ghodsi, et al., 1997; Balk, 1995; Wu et al., 2009).

Tantalum pentoxide is used as a reflective barrier layer in silicon solar cells (Rubio et al., 1982), in optical waveguides (Tu et al., 1987), as a gate insulator in thin-film transistors, in storage capacitors in memory cells (Shinriki et al., 1989; Shinriki et al., 1991), in tuneable mirrors (Tajima et al., 2008; Tajima et al. 2009), as an ion-conductive layer in multilayer electrochromic devices (Wang et al., 2011; Sone et al., 1996), and as a protective layer in electrochromic devices to prevent erosion of liquid or gel electrolytes (Sone et al., 1996; Ahn et al., 2002).

Within the scope of the thesis, Ta_2O_5 thin films were investigated as ion-conductive layers for the production of solid-state electrochromic devices.

2.5. Transparent Conductive Oxides (TCOs)

Transparent conductive oxides (TCOs) are thin films that are electrically conductive and optically transparent. TCO was first discovered by Baedeker in 1906 with CdO thin films (Baedeker, 1906). After this discovery, many transparent conducting oxides are found such as SnO_2, In_2O_3, ZnO, ITO, FTO, ZTO, $Cd_2\ SnO_4$, $CdSnO_3$. Nowadays, transparent conducting oxides materials are commonly used electronic and optics devices such as sensors, solar cells, smart windows, etc. (Jayathilake et al., 2018). Among of these transparent conducting oxides materials, aluminium-doped ZnO (AZO), fluorine-doped SnO_2 (FTO), GZO, tin-doped indium oxide In_2O_3: Sn (ITO) are used to produce various applications frequently (Zeng et al., 2003). However, there are cases where these thin films do not provide the desired performance. For example, AZO, GZO thin films have poor electrical conductivity, and coatings made from FTO thin films have a hazy appearance. The other example, although ITO is the most preferred reason for device production due to it has ~85% optical transmittance at 400-700 nm and high electrical conductivity ($10^4\ \Omega^{-1}\ cm^{-1}$), the scarcity of indium in nature creates a cost disadvantage. (Tuna et al., 2010; Köseoğlu, 2015). Transparent conductive oxides (TCO) are an essential and essential part of many electrochromic devices. Due to their optical and electrical properties, they can affect the efficiency of electrochromic devices (Ekmekcioglu et al., 2021). In this

study, a commercially available ZTO/Ag/ZTO transparent conductive oxide layer electrochromic device was made.

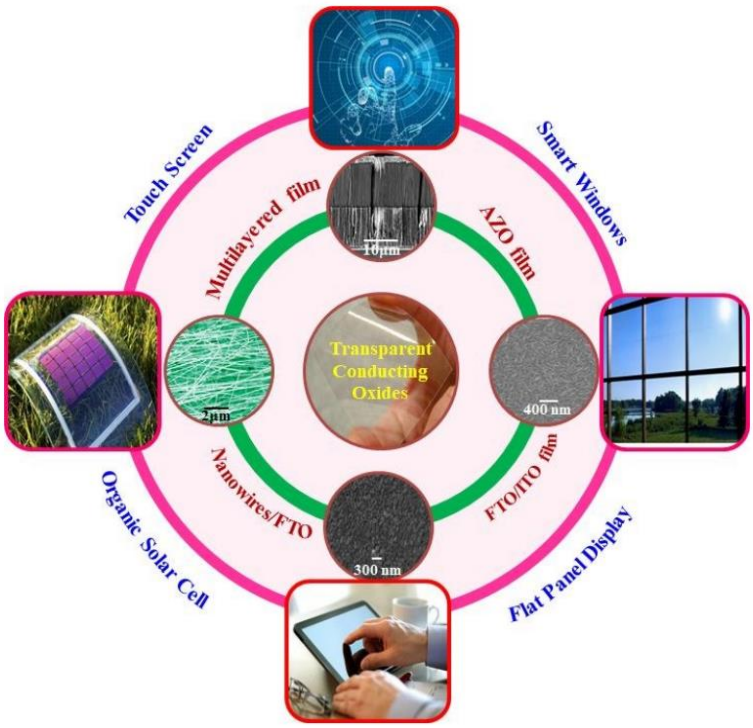

Figure 2.2. Schematic diagram of various transparent conducting oxides and applications (Source; Ghorannevis et al., 2015; Higashitani et al., 2011)

2.6. Properties of Thin-Film ZTO

Zinc tin oxide (ZnSnO or ZTO) is an n-type transparent semiconductor, and it has a wide energy band gap. Stoichiometry of ZTO is expressed as $(ZnO)_x(SnO_2)_{1-x}$ ($0<x<1$). Although the binary oxides ZnO and SnO_2, which are transparent semiconductor materials, have favourable properties, ternary oxides exhibit better properties. In the studies, two crystalline forms of ZTO called ilmenite ($ZnSnO_3$) and cubic spinel (Zn_2SnO_4) have been observed. The ilmenite form has limited thermal stability whereas the decomposition of $ZnSnO_3$ as Zn_2Sn0_4 and SnO_2 has been reported at low temperatures up to 600 °C. Furthermore, Zn_2SnO_4 has a 3.35 eV band gap. For this reason, the Zn_2SnO_4 crystalline form is a unique material with high electron mobility, low visible absorption, and high electrical conductivity (Chiang et al. 2005). ZTO is a good

semiconductor oxide due to its physical properties. However, it is possible to increase the electrical conductivity and use it as an electrode by growing the conductive material Ag between the two zinc tin oxides (zinc tin oxide / Ag / zinc tin oxide or ZAZ/Ag/ZAZ). ZAZ/Ag/ZAZ is shown by Schmidt these multilayer thin films have a sheet resistance of 6 Ω/□, optical transmittance of 82% at 550 nm and a suitable work function of 4.3 eV (Schmidt et al., 2011).

2.7. Electrolyte Materials

This layer allows the ions to reach the electrochromic layer by activating when voltage is applied. The material to be used for the ion conductive layer should have high optical transmittance and ion conductivity, and low electrical conductivity. In electrochromic devices, it can be used in polymer electrolyte as well as different types of electrolytes such as thin film or liquid electrolytes with inorganic ion conductivity. The small diameter of Li^+ ions (K^+, Na^+, H^+ etc.) to be formed in this layer provides ease of movement to the ions and easy ion exchange within the applied electric field (Kraft, 2018).

2.8. Thin Film Deposition Technique

Thin film deposition is the process of applying materials in the form of a thin layer, either atomically or molecularly, onto a surface. This technique is widely used in electronic devices, optoelectronic devices, sensors, energy storage systems, and many other applications. There are several different methods for thin film deposition. Here are some of the most commonly used techniques:

Physical Vapor Deposition (PVD): In this method, the material is vaporized from a source and then condensed onto a surface. PVD includes subcategories such as evaporation and sputtering. These methods are often used for depositing metallic or ceramic materials.

Chemical Vapor Deposition (CVD): In this method, one or more chemical compounds are introduced as gases into a reactor, where they undergo

chemical reactions on the surface to form a thin film. CVD is often preferred for obtaining thin films with high purity and controllable thickness.

Atomic Layer Deposition (ALD): ALD is a method that deposits materials layer by layer to form a film. Each layer consists of sequential steps of adsorption of a chemical compound onto the surface and subsequent purging with an inert gas. This process allows for precise film thickness control and high conformality.

Spin Coating: In this method, the material is prepared as a solution or suspension and applied onto a rotating substrate. The spinning motion spreads the material into a thin film on the surface. Spin coating is a low-cost and simple technique commonly used for depositing organic materials.

Magnetron Sputtering Deposition: Magnetron sputtering is a technique used for thin film deposition. In this process, a target material, typically a solid metal or compound, is bombarded with high-energy ions in a vacuum chamber. The target material is placed in close proximity to a magnetron, which generates a magnetic field. This magnetic field enhances the sputtering process by trapping electrons near the target surface, increasing the ionization efficiency and promoting ion bombardment. The magnetron sputtering technique offers several advantages over conventional thermal spraying methods. It provides better control over film thickness and composition, as well as higher deposition rates. The use of magnetic fields allows for more efficient ionization of gases in the plasma, reducing the need for high temperatures. Additionally, magnetron sputtering enables deposition on complex-shaped substrates and can be used to deposit a wide range of materials, including metals, alloys, semiconductors, and dielectrics.

These are just a few examples and there are many other methods for thin film deposition as shown in the Figure 2.3. below. Each method has its advantages, disadvantages, and specific application areas. Thin film deposition techniques play a significant role in the development of complex and high-performance devices, making them crucial in various industrial and scientific fields (Park et al., 2016).

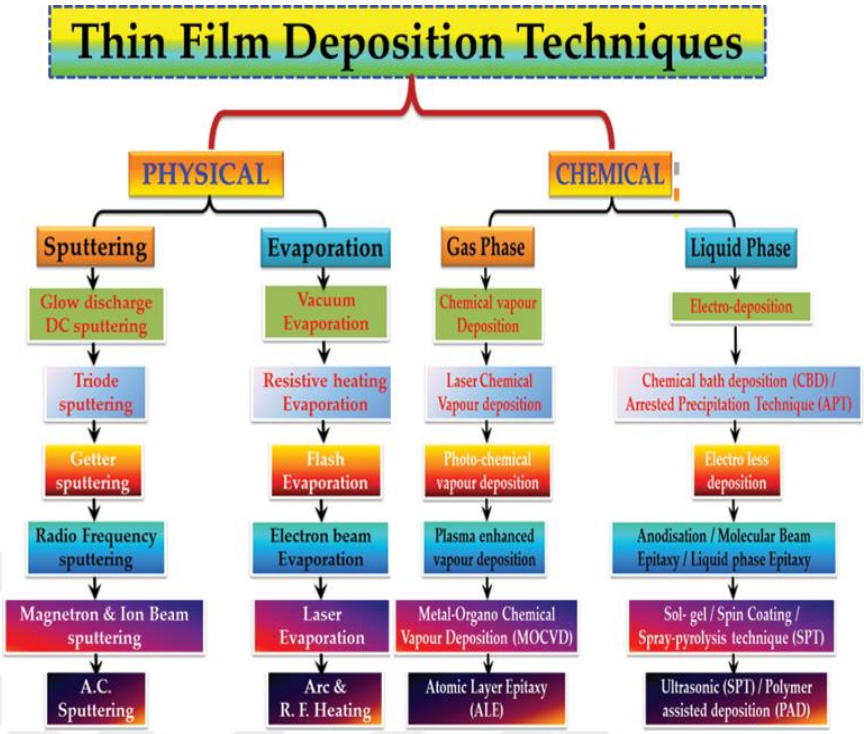

Figure 2.3. Flowchart illustrates the physical and chemical deposition process widespread thin film techniques. (Source: Thirumalai, 2017)

CHAPTER 3

EXPERIMENTAL PROCEDURE

3.1. Magnetron Sputtering

Magnetron sputtering method, which is one of the most common and functional thin film coating methods, has been used for the production of electronic devices. The magnetron sputtering system shown in Figure 3.1. works as follows.

Figure 3.1**.** Magnetron Sputtering System

Magnetron sputtering is the breaking from atoms in the target material and the deposition of these particles on the substrate. Argon gas sent into the magnetron sputtering system becomes an ionized charged particle due to the potential difference between the anode and the cathode. These ions are

accelerated by the electric field effect and gain energy. Ionized particles that reach the threshold energy hit the target material and transfer some of their energy to the particles that make up the target material, causing the particle to break away from the target material. Thanks to the magnetic field created by the magnets under the target materials, the efficiency is increased by directing the ions onto the target material. With this system, multiple layers were deposited on top of each other. In this system, coatings were made by magnetron sputtering method using 3 different targets. In this system, WO_3, Ta_2O_5, NiO_x depositing were made, respectively.

Before deposition, large ITO deposition glasses were cut with a 7x11 cm diamond cutter. The target-to-sample distance was set to 7 cm. Photoresist SLG (Soda Lime Glass) glass was placed next to the 7x11 cm ITO deposited sample to gain thickness. WO_3 and NiO_x thin films were deposited separately on 225 nm thick ITO deposited glasses with resistivity R= 15 Ω/□ and glass size 7x11 cm. Thin film metal oxides were deposited using the reactive DC magnetron sputtering technique using 241.2x84.2x7 mm pure tungsten (99.9% purity) and nickel (99.9% purity) as sputtering gun. First, ITO deposited glasses are placed inside the system. Then the vacuum system was reduced to $7.4x10^{-6}$ hPa base pressure. Ar gas was sent into the system and pre-sputtered for 10 minutes. The purpose of pre-sputter is to clean the particles and dirt that may occur on the target. By sending Ar and O_2 gas into the system, the deposition of WO_3 and NiO_x thin films was carried out with a constant DC power supply. Thin film deposition parameters are given in the table 3.1 below. Ar and O_2 flow rates were controlled with the aid of a mass controller. Thanks to this control, film thicknesses and deposition times can be adjusted. All thin films in this study were deposited in this way.

Table 3.1 Detailed experimental parameters of the WO_3, NiO_x and Ta_2O_5 thin films

Film	Target	Ar/O_2 (sccm)	Working Pressure (hPa)	Power (W)	Sputtering Time (minute)
WO_3	W	68.5/20	$5.4x10^{-3}$	150	15,17.5,30,35
NiO_x	Ni	30/7.5,10,12.5	$5.4x10^{-3}$	50	25
Ta_2O_5	Ta	68.5/5	$5.4x10^{-3}$	125	20,25

Figure 3.2. Plasma of the magnetron sputtering system

3.2. Thickness Measurement by Profilometry

The thickness parameter of the films grown on SLG is an important factor for the device that was produced. In order to measure the roughness of a surface and the thickness of the thin films was used Veeco DEKTAK 150 profilometer which is shown in Figure 3.3. While the tip of the needle in the device scans the surface in three dimensions, the topological difference between the coated and uncoated parts creates data. In this case, an average thickness is determined by the computer.

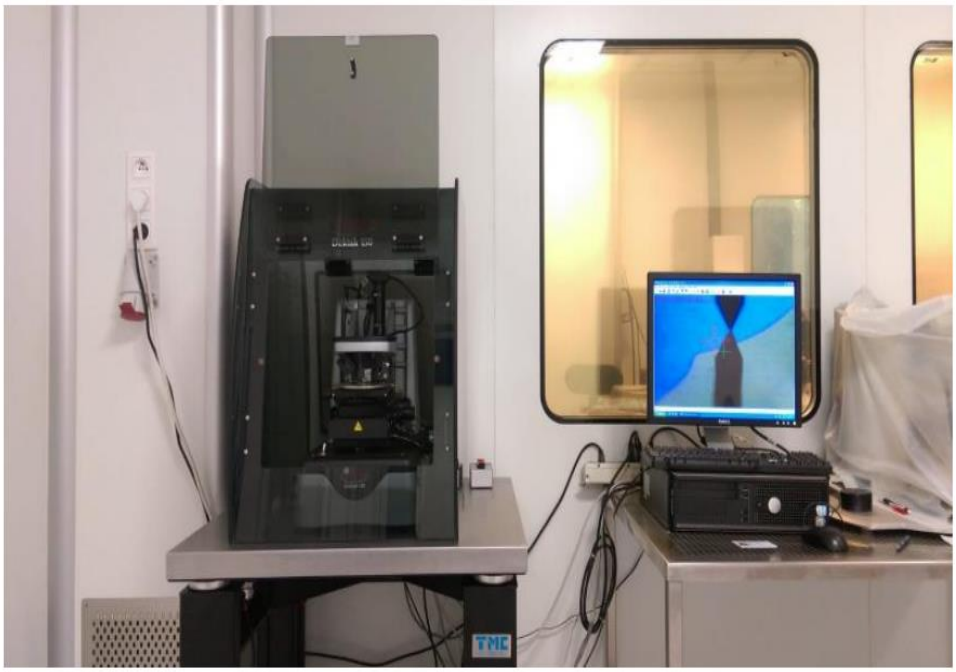

Figure 3.3. The picture of the profilometer

3.3. Optical Transmission

UV/VIS/NIR spectroscopy is a technique to measure the optical properties such as transmittance, absorbance, and reflectance of materials. Optical transmittances of the above-mentioned coatings were measured via PerkinElmer Lambda 950 UV/VIS/NIR portable spectrophotometer which is represented in the Figure 3.4. The spectral range for measurement is from 200 to 2600 nm.

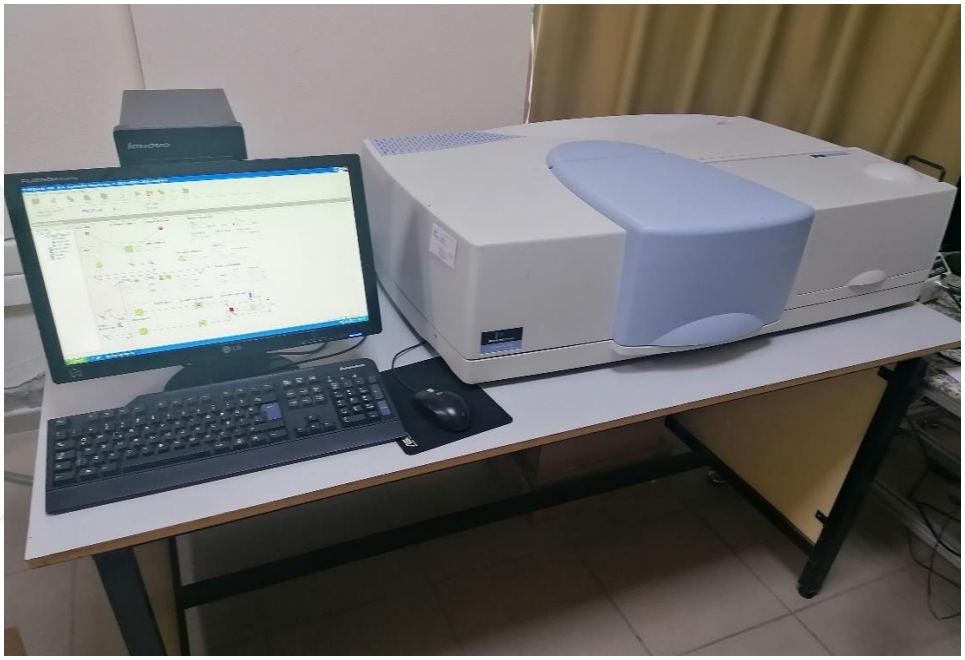

Figure 3.4**.** The picture of PerkinElmer Lambda 950 UV/VIS/NIR portable spectrophotometer

3.4. Scanning Electron Microscopy (SEM)

SEM has recently become a key technology in the morphological characterization of materials. It is used in the characterization of properties such as grain boundaries, porosity, and surface morphology of thin films by SEM method (Moorthy, 2015).

Figure 3.5. Research room of scanning electron microscopy (SEM)

3.5. Structure Analysis by XRD

One of the most used methods to describe the crystal structure of materials is XRD. Thanks to this method, together with the crystal structure of the material; Information such as distances between atoms or planes, lattice shape and size can also be accessed. The wavelength range corresponding to X-rays in the electromagnetic spectrum is 0.1-100Å. The wavelengths used in XRD are 1 Å and this value is equal to the distance between the crystal atoms. For this reason, X-rays are used in crystal structure determination (Moorthy,2015).

3.6. Electrochemical Characterization of Electrodes

Electrochemistry is the science that studies the interaction of matter with electrical energy and the resulting chemical transformations and physical changes and the conversion of chemical energy into electrical energy. Electrical quantities such as current, potential and charge are measured and their relationship with chemical parameters is found. Electrical quantities such as current, potential and charge are measured and their relationship with chemical parameters is found. Solutions of salts, inorganic acids and bases in water or other suitable solvents conduct electricity. Such solutions are called electrolytes. The transmission of electricity with the help of a liquid is called electrolytic conductivity. If metal sheets called electrodes are dipped into aqueous solutions of acids, bases or salts and these metals are connected to a power source, it is seen that current flows through the solution and some electrochemical reactions take place. Chemical reactions due to current usually take place at the interface between the electrode and the solution (Choudhary et. al., 2017).

The metal plates forming the poles of the external circuit are called electrodes, the electrode connected to the positive pole of the power source is called the anode, and the electrode connected to the negative pole of the power source is called the cathode. In an electrochemical cell, a reduction reaction occurs at the cathode and an oxidation reaction occurs at the anode.

In an electrochemical cell, the study of the cell potential change is called "potentiometry", and the study of the current change in the cell is called "voltammetry". In this thesis, cyclic voltammetry (CV) and chronoamperometry (CA) techniques were used.

Three-electrode system is commonly used in voltammetry measurements. These electrodes consist of counter electrode, reference electrode, and working electrode. The counter electrode is also known as the "auxiliary electrode". It is used to complete the current circuit in the electrochemical cell. Prime materials such as Pt, Au, graphite, glass carbon is used. The reference electrode is a stable electrode with a known electrode potential. It is used as a reference in the control and measurement of the potential of the electrochemical cell. The current through the reference electrode is ideally zero. The working electrode is the electrode on

which the chemical reaction will be examined (Elgrishi et. al., 2018). In this thesis, ITO-ZAZ thin films and multilayer coatings, whose electrochromic properties will be examined, are working electrodes. Figure 3.6. shows the electrochemical deposition technique.

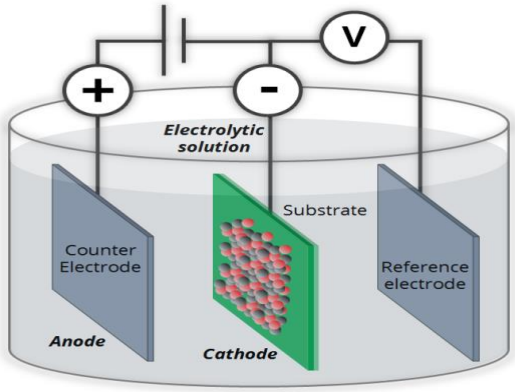

Figure 3.6. Scheme of electrochemical deposition technique (Source; Park et al., 2016)

In order to evaluate the electrochemical performance during the insertion/extraction of Li^+ ions, their values were recorded with CV and CA programs. Electrochemical characterizations were performed for glass/ITO/WO_3, glass/ITO/NiO_x and glass/ITO/WO_3/Ta_2O_5 films. The potentiostat/galvanostat was performed in a conventional three-electrode cell using the Gamry 600 electrochemical workstation. Previous studies have shown that $LiClO_4$-PC electrolyte is suitable for WO_3 and NiO_x thin films. The electrodes are immersed in a 1M $LiClO_4$ electrolyte solution in propylene carbonate (PC), which provides mobile Li^+ ions. CV tests, potential range of -1.0 and 1.0 mV/s and -0.6 and 1.2 mV/s for WO_3 and NiO_x thin films, respectively was carried out at a scanning rate of 100 mV/s.

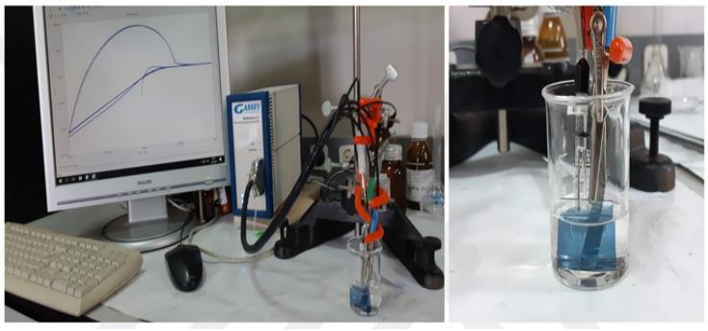

Figure 3.7. The CV work chart is shown on the left. On the right, the 3-electrode electrochemical characterization is shown

3.7. Cyclic Voltammetry (CV)

If the voltage applied to an electrochemical cell is in one direction, that is, if the applied voltage is constantly increasing or decreasing at a certain scanning rate, it is called linear voltammetry. The scanning rate here indicates the value of the voltage to be applied depending on time. If the applied voltage returns to its initial value with a certain scanning rate, it is called cyclic voltammetry. The variation of the voltage applied to the cell with time in Cyclic Voltammetry is as in figure 3.8. With the measurement made, the function of this voltage current is obtained (Figure 3.9.). With cyclic voltammetry measurements, which is a method used to understand the kinetics of redox reactions, cathodic or anodic peak currents are determined depending on the type of material. The magnitude of the peak current obtained from the CV curves varies with the concentration of the electroactive substance, the number of transferred electrons, the electrode surface area, and the diffusion coefficient (Kim et.al., 2020).

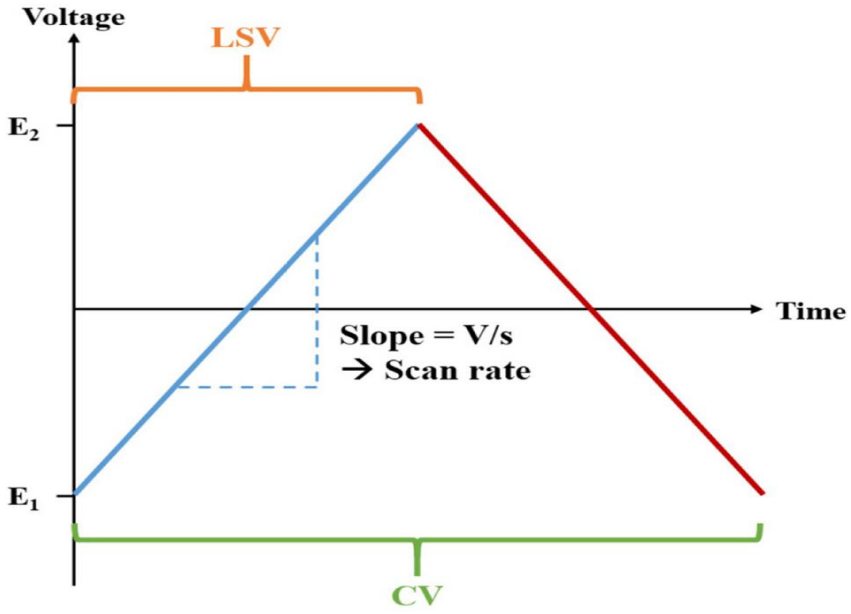

Figure 3.8. Variation of applied voltage with time in cyclic voltammetry (Source; Kim et.al., 2020)

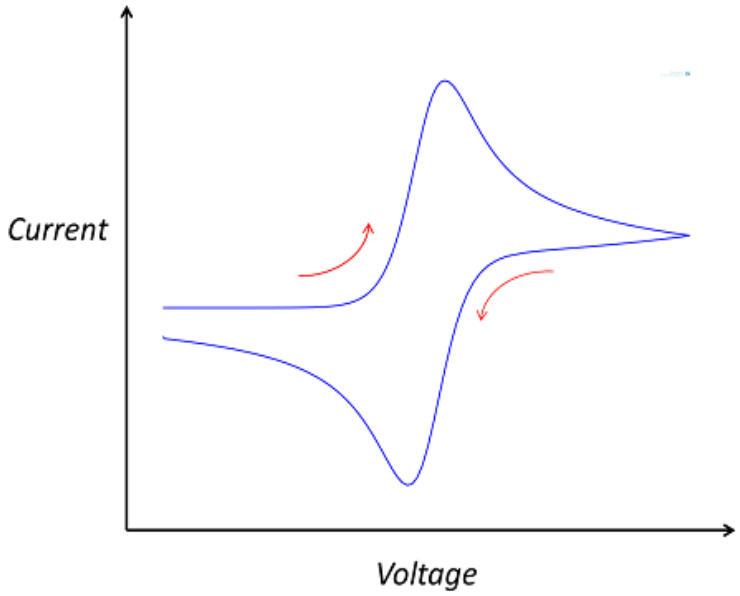

Figure 3.9. Schematic representation of a typical voltammogram in CV (Source; Forrister, 2018)

In order to examine the electrochemical properties of the electrochromic thin film, the ion input and output processes are performed with cyclic voltammetry measurements. Depending on the polarity of the applied potential, ions and electrons are added and removed from the structure. Using the information obtained from the CV curves, the amount of charge insertion/extraction the material (cathodic/anodic charge amounts) and the ion storage percentage of the material are calculated (Forrister, 2018).

3.8. Chrono Amperometry (CA)

The voltammetry type, which examines the time-dependent step potential versus the time-dependent step potential applied to the cell, is called chronoamperometry (CA) measurement. In Figure 3.10., chronoamperometry is used to investigate electrolysis, metal deposition and electrochemical system analysis and their stability over time.

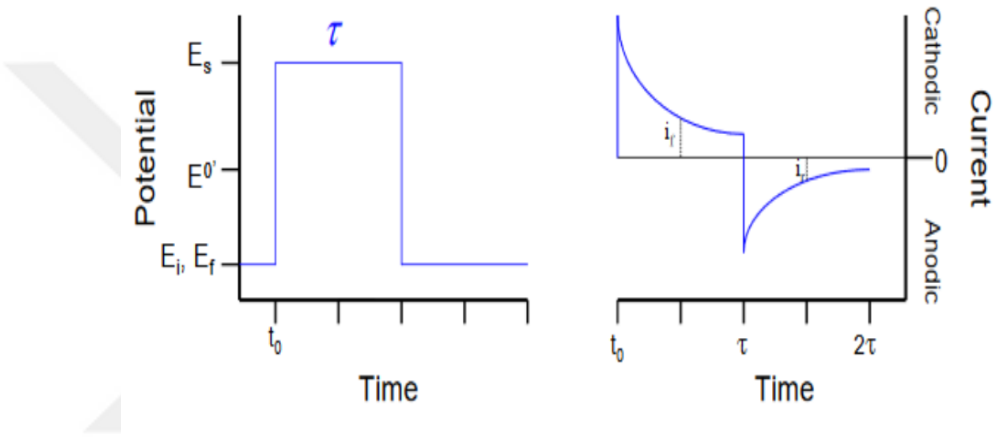

Figure 3.10. Excitation waveform and response waveform in chrono amperometry (Source; Forrister, 2018)

For electrochromic reactions, the anodic and cathodic current values, the amount of charge insertion/extraction the film, and the areas under the current time curve are calculated from the CA measurement. The coloration efficiency of the film can be calculated by utilizing the obtained load amount values (Forrister, 2018).

3.9. Electrochemical Impedance Spectroscopy (EIS)

Electrochemical Impedance Spectroscopy (EIS) is an experimental technique used to investigate the electrical interactions on the electrode surface in electrochemical systems. This technique is commonly employed to understand the interactions between the electrolyte and the electrode in electrochemical cells. EIS analyzes the relationship between voltage and current on the electrode surface in a frequency spectrum. This spectrum consists of both amplitude and phase spectra. The amplitude spectrum represents the magnitude of voltage or current as a function of frequency, while the phase spectrum represents the phase difference between voltage and current. These spectra are used to determine the nature and kinetic properties of electrochemical interactions on the electrode surface (Li et al., 2018). The fundamental principle of EIS arises when an alternating current is applied to the electrochemical system. The frequency of this current typically varies over a wide range and helps to determine the system's response to electrochemical interactions within the frequency range. Electrical equivalent circuit models are commonly used to assess the complexity of electrical interactions on the electrode surface. EIS is widely used in the characterization of electrochemical systems, electrochemical research, and materials science. It serves as an important research tool in various fields, particularly in the performance analysis of electrochemical cells, electrode material selection, and surface modification (Pajkossy, 2020).

CHAPTER 4

RESULT AND DISCUSSION

4.1. ZTO/Ag/ZTO (ZTO= Zn_2SnO_4) Physical Properties

The reasons why ZTO/Ag/ZTO(ZAZ) thin films can be used instead of ITO is that they have better optics and better electrical conductivity. Therefore, it can be used as a transparent conductive oxide in electrochromic structures.

Table 4.1. Deposition parameters of ZAZ thin films of different power on glass

Sample Number	Ar (sccm)	Power (W)	Voltage (V)	Current (A)	Sheet Resisdance (Ohm/square)	Transmission (%) (λ=550 nm)
K-017-ZAZ	137	50/75/50	254/339/253	0.27/0.29/0.27	5.78	72.9
K-018-ZAZ	137	50/60/50	255/329/255	0.27/0.25/0.27	7.32	79.6
K-019-ZAZ	137	50/40/50	254/317/256	0.27/0.20/0.27	14.28	83.9
K-020-ZAZ	137	50/45/50	253/320/254	0.27/0.21/0.27	11.19	83.5
K-021-ZAZ	137	50/45/50	255/319/255	0.27/0.21/0.27	10.76	84.5

4.1.1. ZTO/Ag/ZTO (ZTO= Zn_2SnO_4) Optical Properties

As the amount of Ag power increases, the transmittance percentages of ZAZ deposited thin films also decrease. Figure 4.1. shows the transmittance graphs of ZAZ deposited thin films.

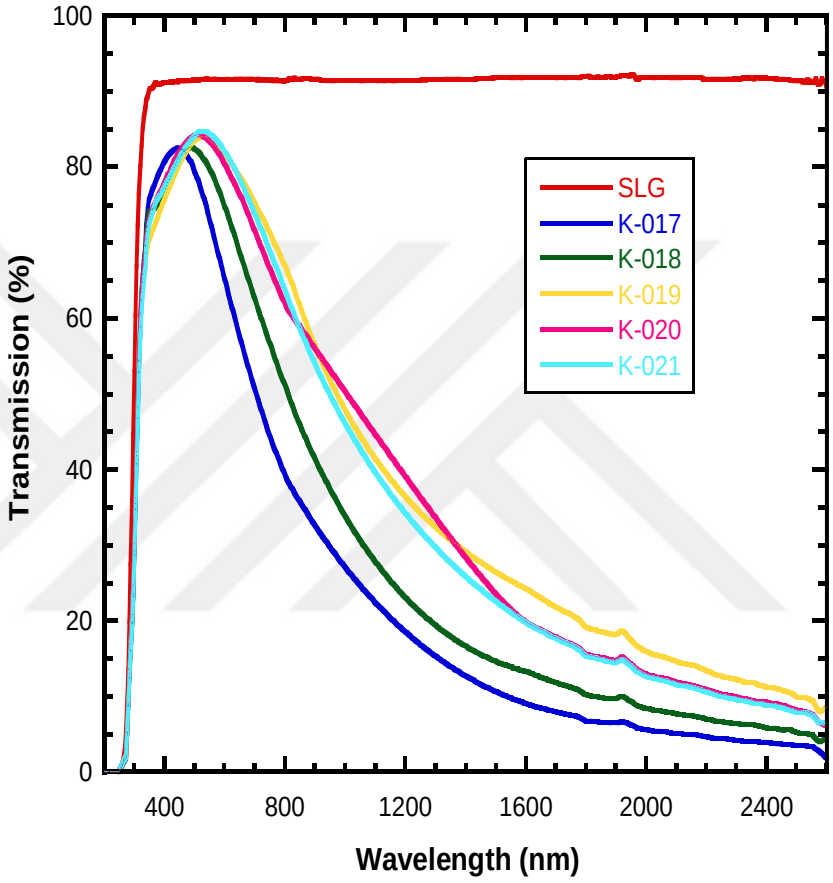

Figure 4.1. Transmittance graph of ZTO/Ag/ZTO samples

Figure 4.2. ZTO/Ag/ZTO coated on 2 mm thick glass

4.2. Tungsten Oxide Physical Properties

It is well known that the ion insertion/extraction of WO_3 thin films is good, and their optical properties work reversibly in electrochromic devices. In this study, transparently deposited WO_3 thin films were obtained. Here, different thicknesses and their transmittance percentages for WO_3 thin films are given in table 4.2.

Table 4.2. Thickness of WO_3 thin films with different deposition times substrate

Sample Number	Ar/ O_2 (sccm)	Power (W)	Deposition Time (min)	Working Pressure (hPa)	Thickness (nm)	Average Transmission (%) (λ=400-700 nm)
WO_3-1	68.5/20	150	15	$5.4x10^{-3}$	176	82.87
WO_3-2	68.5/20	150	17.5	$5.4x10^{-3}$	204	78.27
WO_3-3	68.5/20	150	30	$5.4x10^{-3}$	352	81.27
WO_3-4	68.5/20	150	35	$5.4x10^{-3}$	387	80.33

4.2.2. Indium Tin Oxide-Tungsten Oxide Physical Properties

WO_3 thin films previously coated on the glass surface were then deposited onto glass/ITO coated thin films. The coating parameters of glass/ITO/WO_3 samples and the average transmittance percentages at 400-700nm are given in table 4.3.

Table 4.3. Deposition parameters of WO_3 thin films with different deposition times on the glass/ITO surface

Sample Number	Ar/ O_2 (sccm)	Power (W)	Deposition Time (min)	Working Pressure (hPa)	Thickness (nm)	Average Transmission (%) (λ=400-700 nm)
ITO-WO_3-1	68.5/20	150	15	$5.4x10^{-3}$	225/176	79.4
ITO-WO_3-2	68.5/20	150	17.5	$5.4x10^{-3}$	225/204	77.8
ITO-WO_3-3	68.5/20	150	30	$5.4x10^{-3}$	225/352	80.4
ITO-WO_3-4	68.5/20	150	35	$5.4x10^{-3}$	225/387	79.1

4.2.3. Tungsten Oxide Optical Properties

The transmittance graphs of WO_3 thin films of different thicknesses coated on glass are given in Figure 4.5. In the graph here, the transmittance values of our glass surface deposited glass are compared. As the thickness of the WO_3 thin film increases, the wavelengths also increase. Figure 4.3 shows a sample of WO_3 coated thin films.

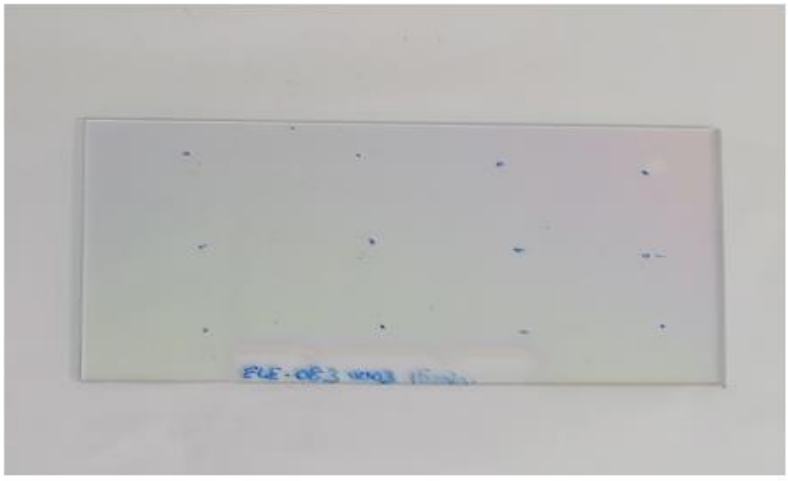

Figure 4.3. WO_3 -1 coated glass

The shape of the thickness map of the WO_3 coated thin film with the OriginPro graphics and analysis program is given in Figure 4.4.

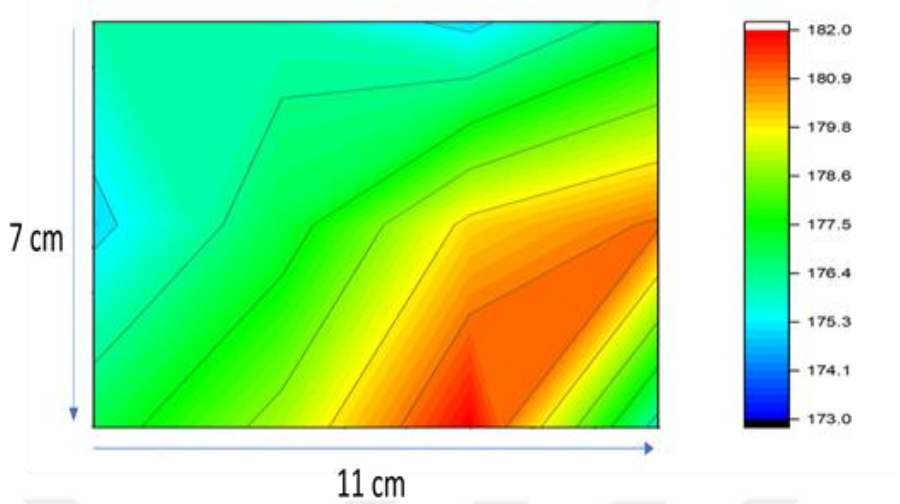

Figure 4.4. WO_3-1 thickness mapping

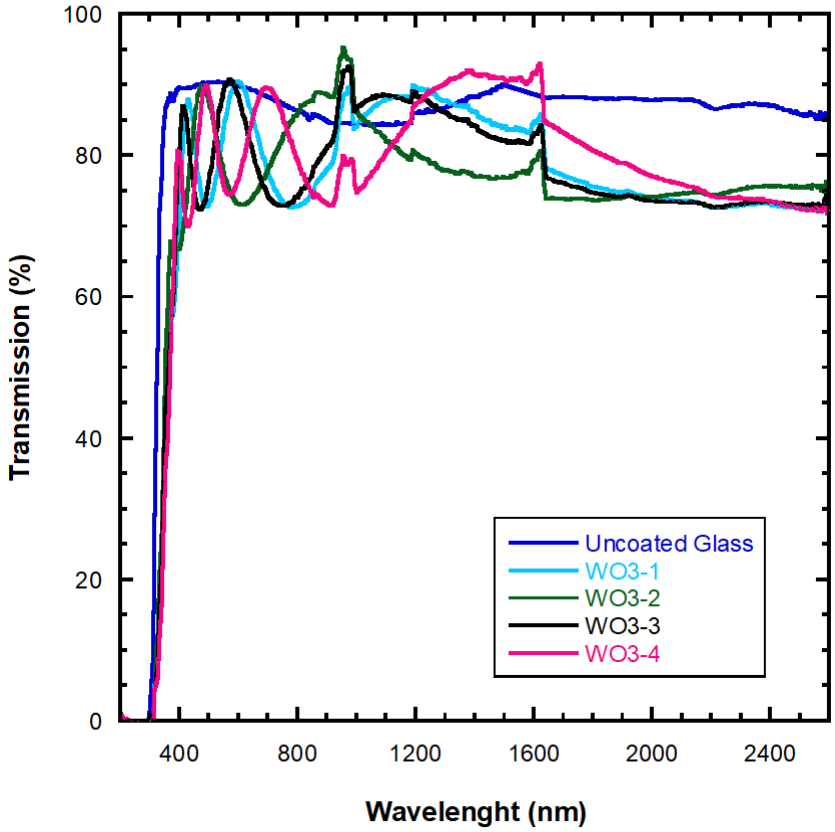

Figure 4.5. Transmittance graphs of glass/WO_3 deposited thin films

4.2.4. Indium Tin Oxide-Tungsten Oxide Optical Properties

Figure 4.6. shows the WO_3 thin film deposited on 7x11 cm glass/ITO. There is 1 photoresist drop SLG glass next to the 7x11 cm glass/ITO coated glass. In this way, the thickness parameter of WO_3 thin film coated on glass/ITO can be found.

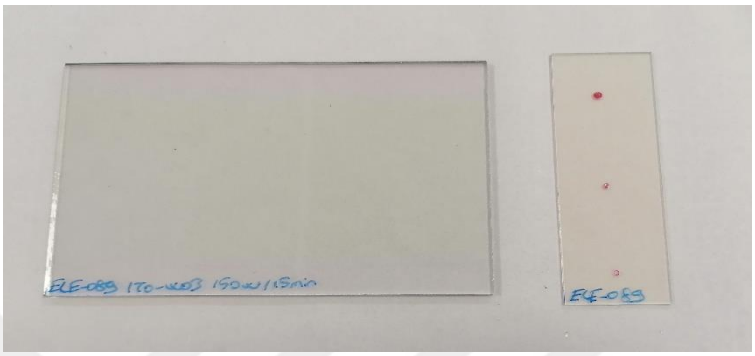

Figure 4.6. ITO-WO_3 -1 coated glass

The transmittance graphs of glass/ITO/WO_3 samples of different coating times are shown in Figure 4.7. In this graph, a comparison was made with the transmittance graphs of only ITO and uncoated glass samples.

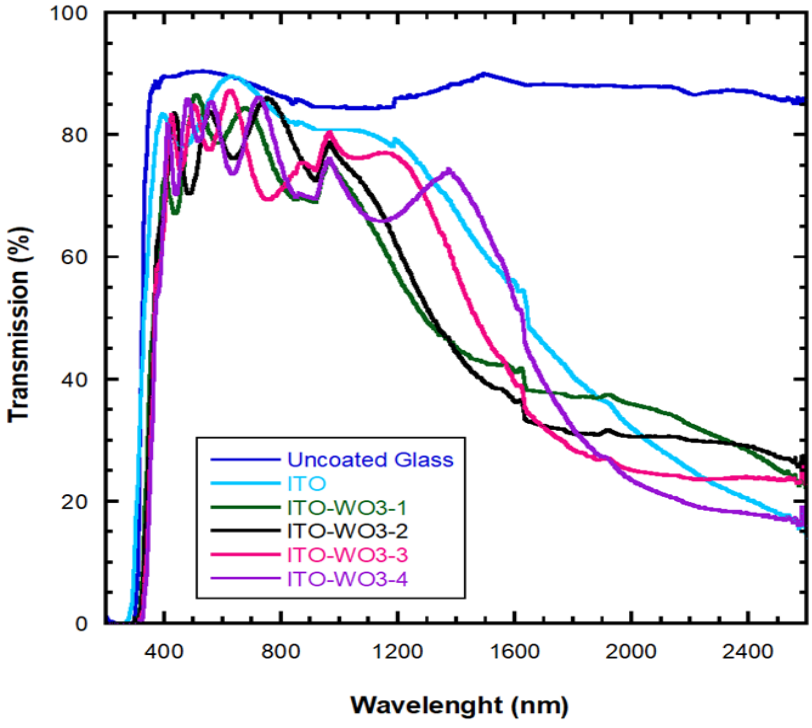

Figure 4.7. Transmittance graph of ITO-WO_3 samples

In Figure 4.8. the color change of glass/ITO/WO_3 coated thin film in 1 M $LiClO_4$-PC electrolyte is shown.

Figure 4.8. Coloration status of glass/ITO/WO_3 deposited thin film in 1 M $LiClO_4$-PC electrolyte

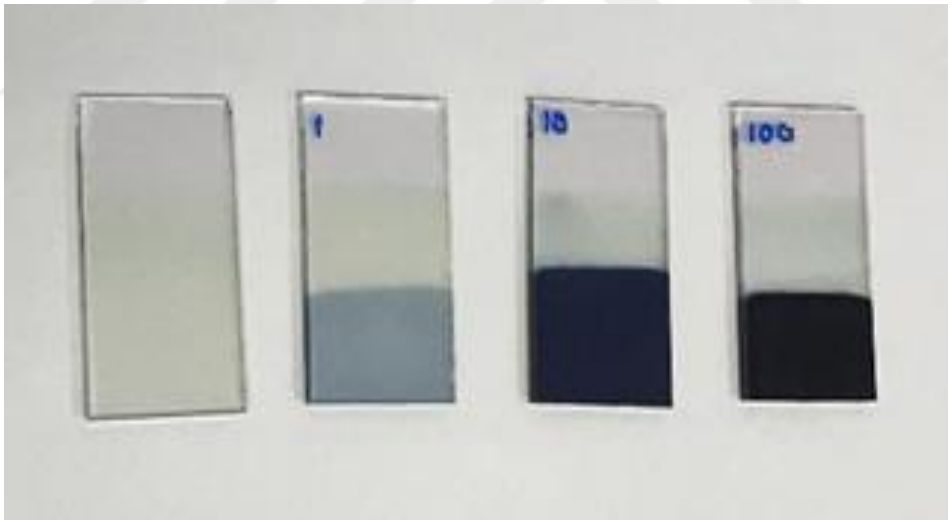

Figure 4.9. Color change of 1-10-100 cycles of glass/ITO/WO_3

Figure 4.9. shows the glass/ITO/WO_3 coated sample and the coloring status of the 1,10 and 100 CV cycles of this sample. The current-voltage graph of the glass/ITO/WO_3 coated thin film sample formed by making 1,10 and 100 CV cycles is given in figure 4.10.

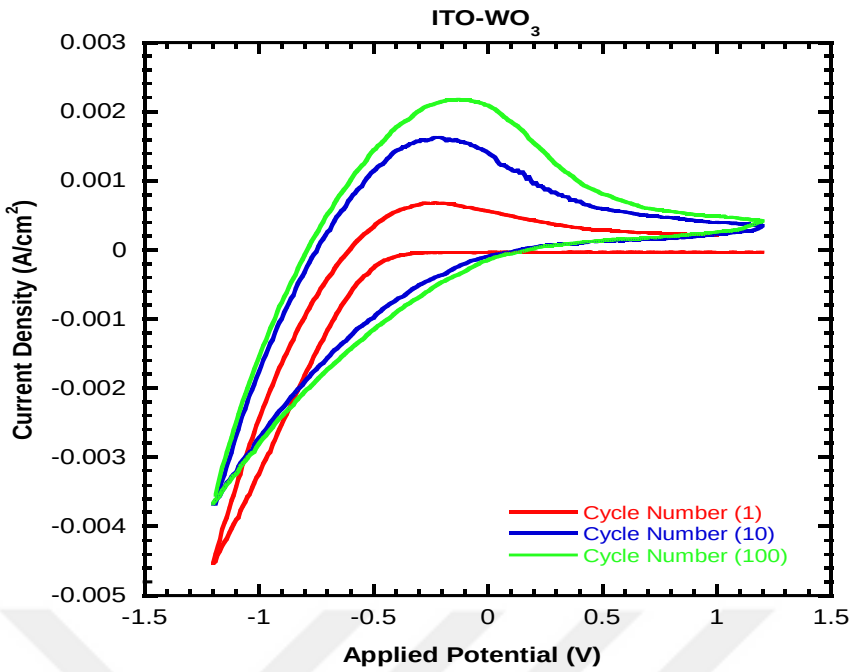

Figure 4.10. Current-voltage graph made by electrochemical CV cycling of WO_3 thin film deposited on ITO.

In Figure 4.11. the transmittance graphs of the bleached and coloration states of the glass/ITO/WO_3-1 coated thin film are given. Here, the comparison is made because the use of glass/ITO/WO_3-1 sample gives the best results in bleaching and coloration conditions.

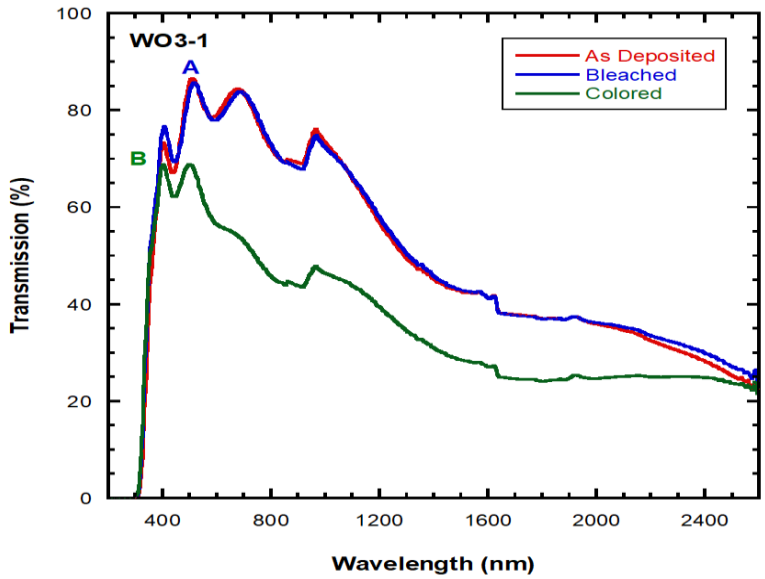

Figure 4.11. Optical transmission graph of the as-deposited, bleached and colored versions of WO_3-1 sample

4.2.5. Indium Tin Oxide-Tungsten Oxide Electrochemical Properties

WO_3 thin film samples were electrochemically tested in 1 M $LiClO_4$-PC electrolyte in the potential range of -1.0 and 1.0 V. Figure 4.12. shows the voltammogram at a scanning rate of 100mV/s. As observed with WO_3 thin films, the higher the film thickness, the more current flows through the thin film and thus the higher the anodic and cathodic peak current densities.

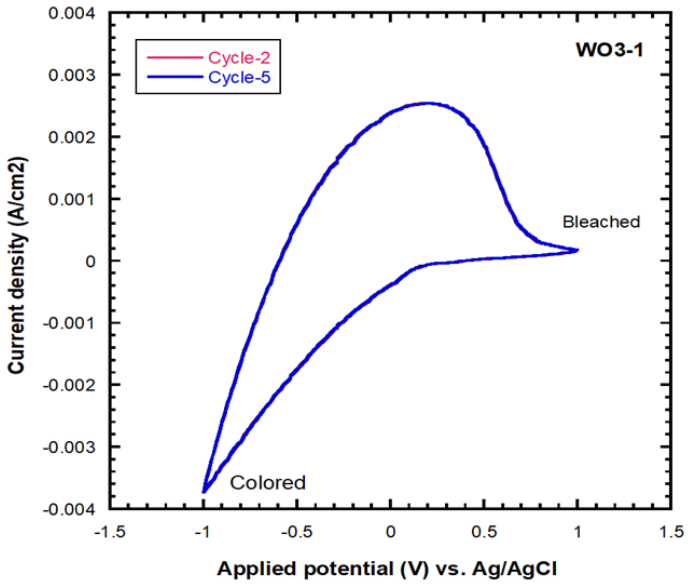

Figure 4.12. Current-voltage graph made by electrochemical CV cycling of WO_3 thin film deposited on ITO. 2 and 5 cycles for the WO_3-1 sample

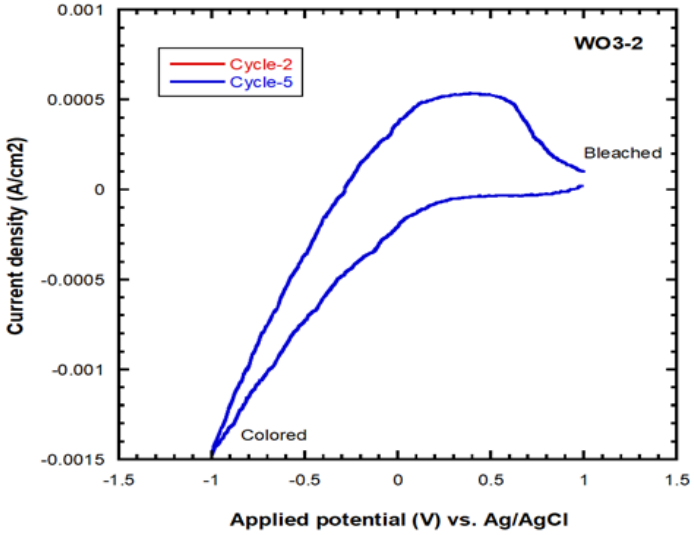

Figure 4.13. Current-voltage graph made by electrochemical CV cycling of WO_3 thin film deposited on ITO. 2 and 5 cycles for the WO_3-2 sample

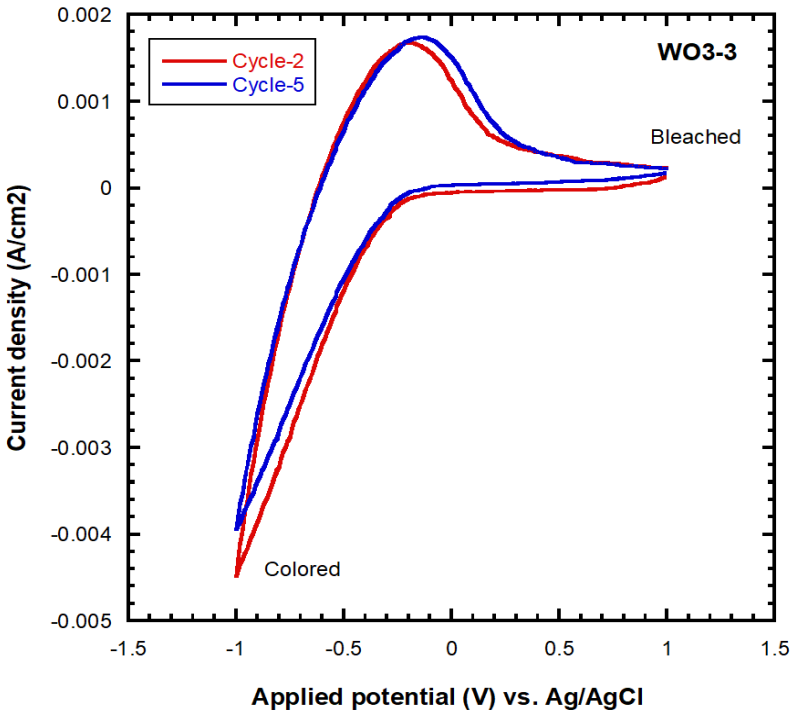

Figure 4.14. Current-voltage graph made by electrochemical CV cycling of WO_3 thin film deposited on ITO. 2 and 5 cycles for the WO_3-3 sample

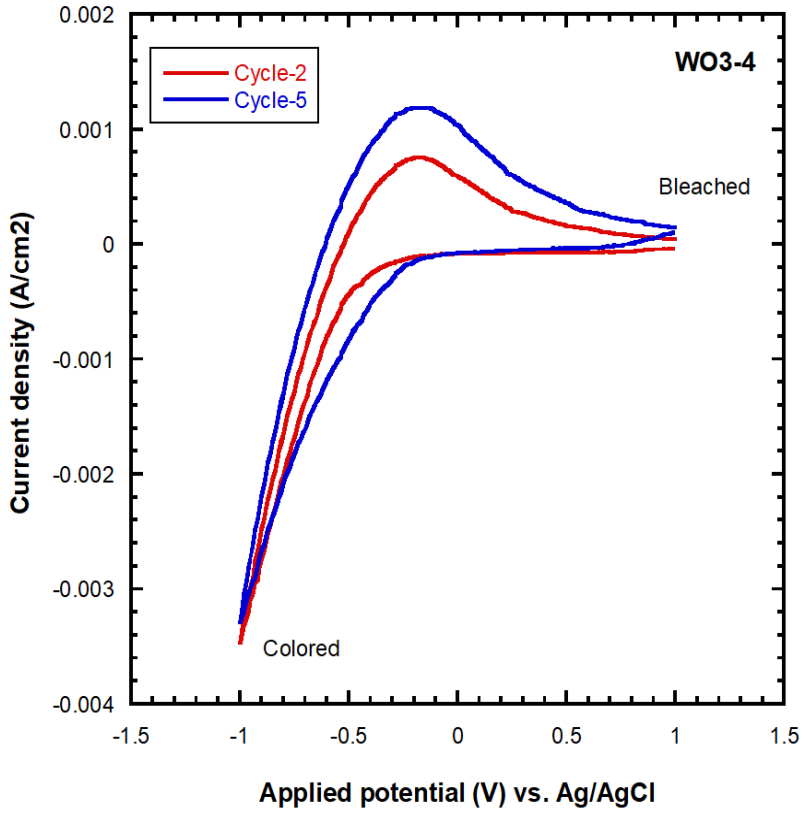

Figure 4.15. Current-voltage graph made by electrochemical CV cycling of WO_3 thin film deposited on ITO. 2 and 5 cycles for the WO_3-4 sample

When the CV cycle graphs of WO_3 thin films of different thicknesses are compared, it is seen that the best result belongs to the WO_3-1 sample. Here, it was observed that as the WO_3 thickness increases, the reversible color change of the film slows down and causes more darkening. What is important here is the stable and continuous color change of our glass/ITO/WO_3 film.The suitable WO_3-1 sample was then tested in higher number of cycles and the current-voltage graph was examined. In Figure 4.16. WO_3-1 example, 250 cycles were made at -1.0 and 1.0 V and 100mV/s.

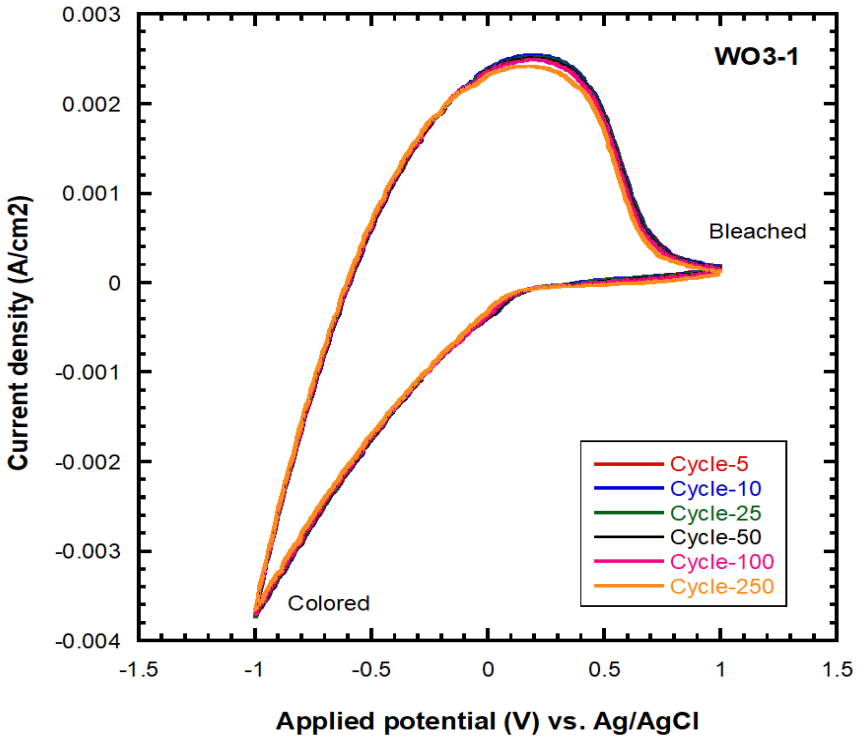

Figure 4.16. Graph of 250 cycles at -1.0 and 1.0 V and 100mV/s for the WO_3-1 sample

Therefore, the charge capacity depends on the thickness of the sample, and as the number of cycles is increased, the addition of Li^+ ions increase depending on the increase in the thickness of the sample.

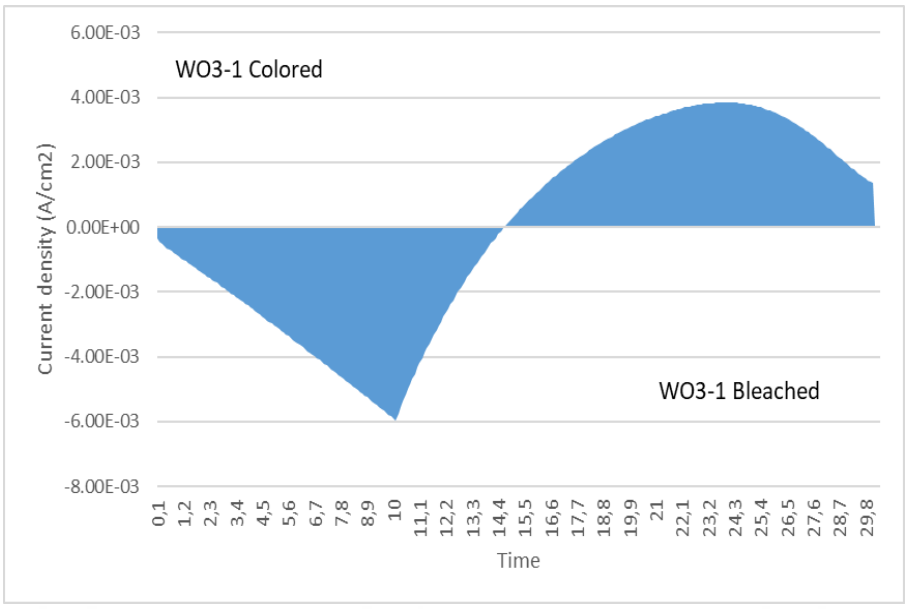

Figure 4.17. Development of current density based on CV measurement of 30 second cycle of WO_3-1 thin film at 100 mV/s

Figure 4.18. Development of current density based on CV measurement of 30 second cycle of WO_3-2 thin film at 100 mV/s

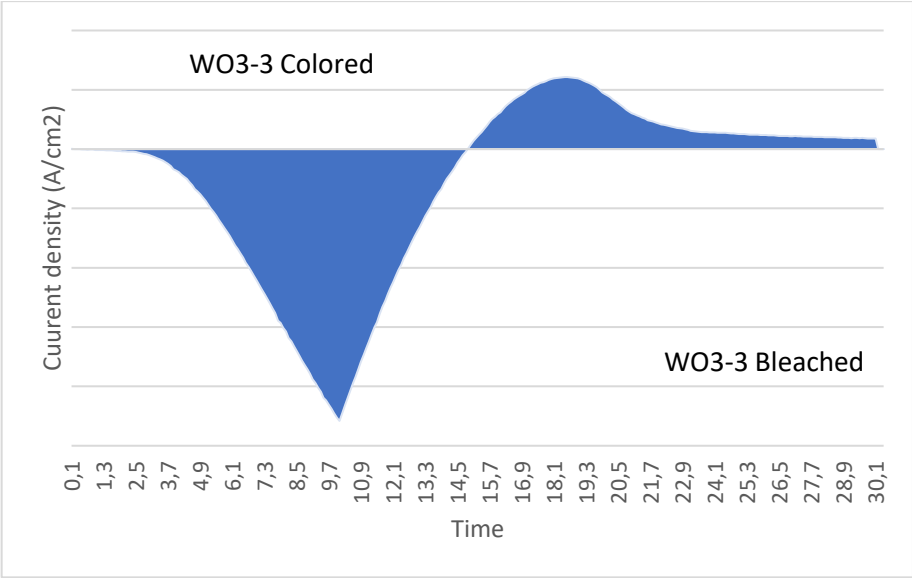

Figure 4.19. Development of current density based on CV measurement of 30 second cycle of WO_3-3 thin film at 100 mV/s

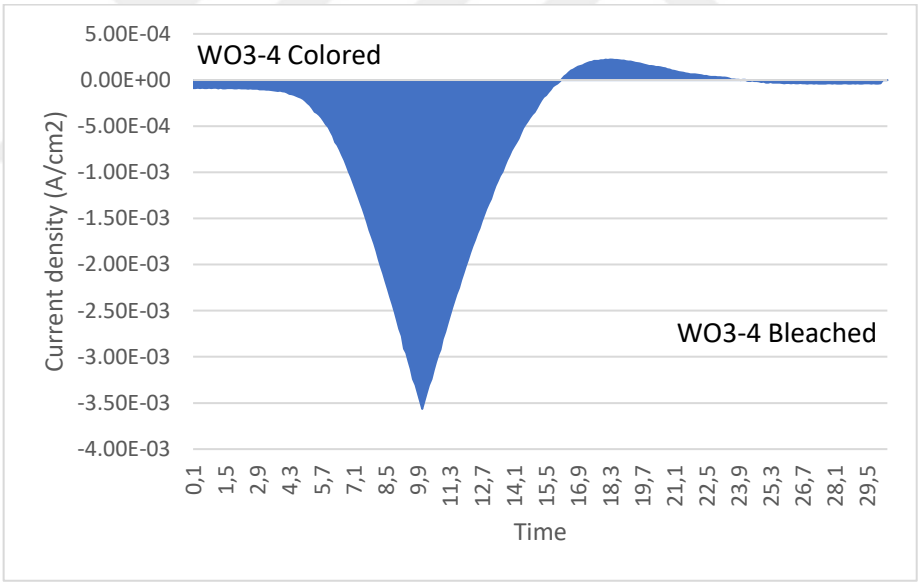

Figure 4.20. Development of current density based on CV measurement of 30 second cycle of WO_3-4 thin film at 100 mV/s

It is seen in the graphs that when the thickness of WO_3 thin films in the time-based cycle increases, the current they draw is also high. As the thickness of WO_3 thin films increases, their coloration also increases, because more Li^+ ions enter the WO_3 thin films. The best bleaching condition is the WO_3-1 example

found in Figure 4.17. Since the WO_3-4 thin film in Figure 4.20. has the highest thickness, its coloration is the highest, but the bleaching condition is the least.

4.3. Nickel Oxide Physical Properties

It is known that the deposited electrochromic NiO_x thin films exhibit an intermediate optical state between the bleached and colored states, which is irreversible under the insertion/extraction of ions. In this study, electrochromic NiO_x thin film was obtained. Table 4.4. shows the thicknesses corresponding to the different deposition times determined by surface profilometry.

Table 4.4. Thicknesses of NiO_x thin films with different deposition times on glass

Sample Number	Ar/ O_2 (sccm)	Power (W)	Deposition Time (min)	Working Pressure (hPa)	Thickness (nm)	Average Transmission (%) (λ=400-700 nm)
NiO_x-1	30/7.5	50	25	$5.4x10^{-3}$	100	27.86
NiO_x-2	30/10	50	25	$5.4x10^{-3}$	107	23.12
NiO_x-3	30/12.5	50	25	$5.4x10^{-3}$	111	21.43

4.3.1. Indium Tin Oxide-Nickel Oxide Physical Properties

Table 4.5 shows the coating parameters of glass/ITO/NiO_x samples with different O_2 gas densities. The average transmittance percentages in the 400-700 nm range of these samples are also given.

Table 4.5. Deposited parameters of glass/ITO/NiO_x samples of different O_2 gas densities

Sample Number	Ar/ O_2 (sccm)	Power (W)	Deposition Time (min)	Working Pressure (hPa)	Thickness (nm)	Average Transmission (%) (λ=400-700 nm)
ITO-NiO_x-1	30/7.5	50	25	$5.4x10^{-3}$	225/100	35.08
ITO-NiO_x-2	30/10	50	25	$5.4x10^{-3}$	225/107	43.43
ITO-NiO_x-3	30/12.5	50	25	$5.4x10^{-3}$	225/111	37.84

4.3.2. Nickel Oxide Optical Properties

NiO_x coated SLG samples are shown in Figure 4.21. Figure 4.22. shows the transmittance graphs of the NiO_x coated samples. Here, our transmittance percentage decreases depending on the thickness of the NiO_x coated thin films.

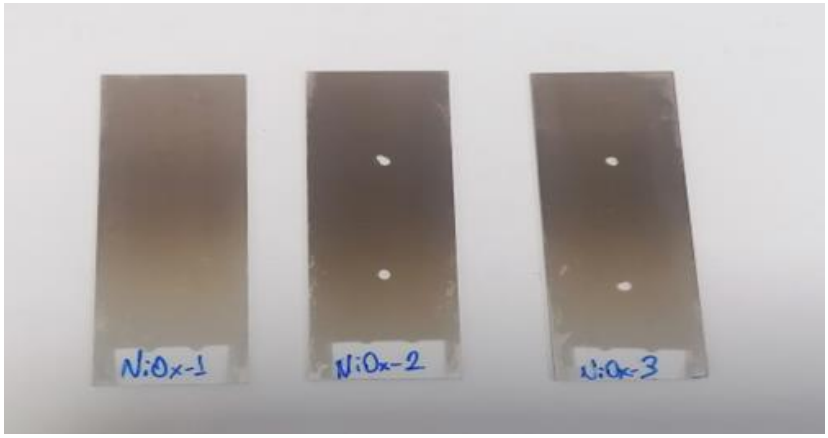

Figure 4.21. NiO_x coated glass

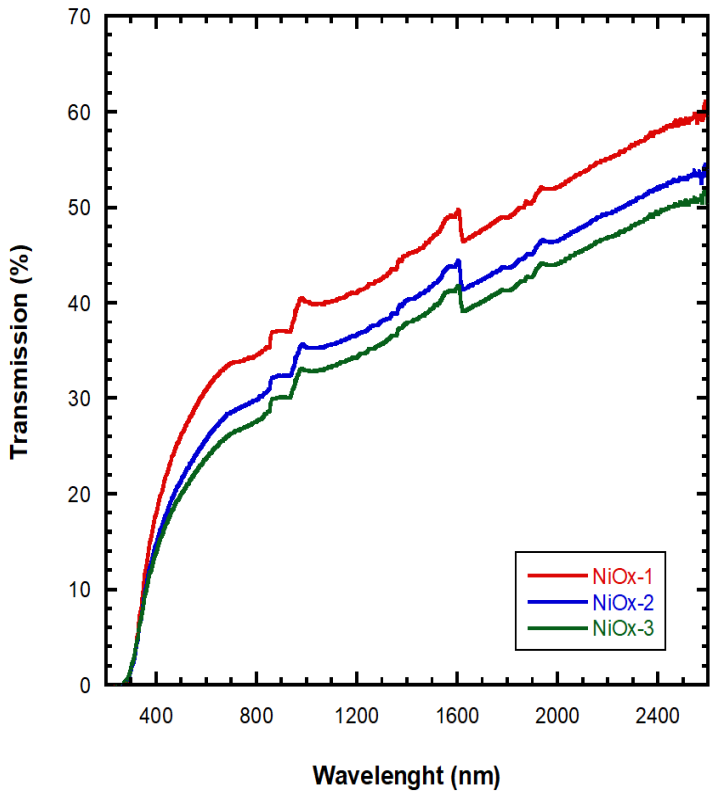

Figure 4.22. Transmittance graphs of NiO_x samples

4.3.3. Indium Tin Oxide-Nickel Oxide Optical Properties

Figure 4.23. shows the NiO_x thin film deposited on 7x11 cm glass/ITO. Figure 4.24. shows the transmittance graph of glass/ITO/NiO_x coated thin film samples compared with ITO and uncoated glass.

Figure 4.23. ITO-NiO_x coated glass

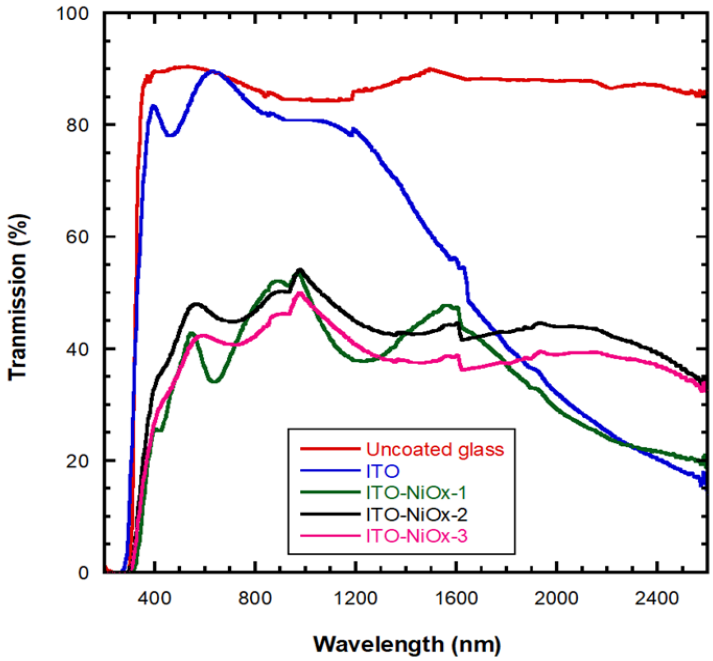

Figure 4.24. Transmittance graphs of glass/ITO/NiO_x deposited thin film

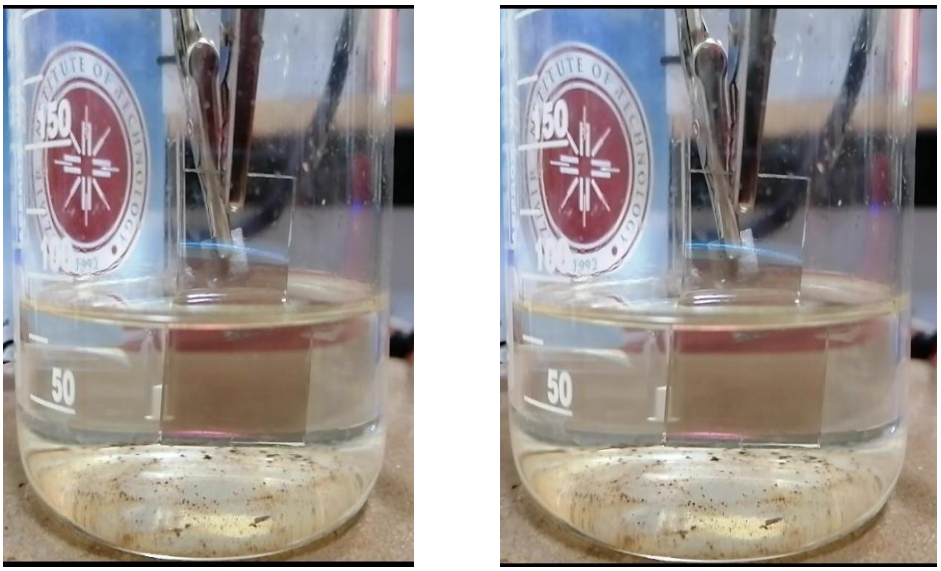

Figure 4.25. Coloration status of glass/ITO/NiO_x deposited thin film in 1 M $LiClO_4$-PC electrolyte

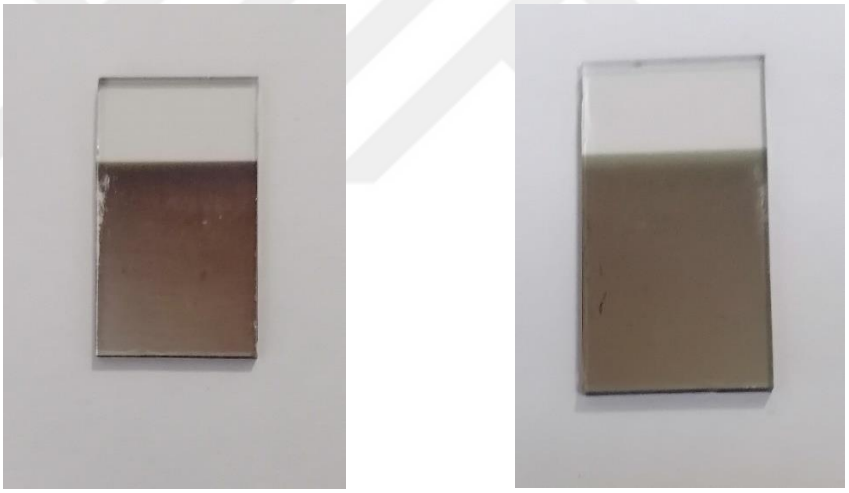

Figure 4.26. Showing the bleached and colored states at -0.6 and 1.2 V and 100mV/s for the NiO_x-1 sample

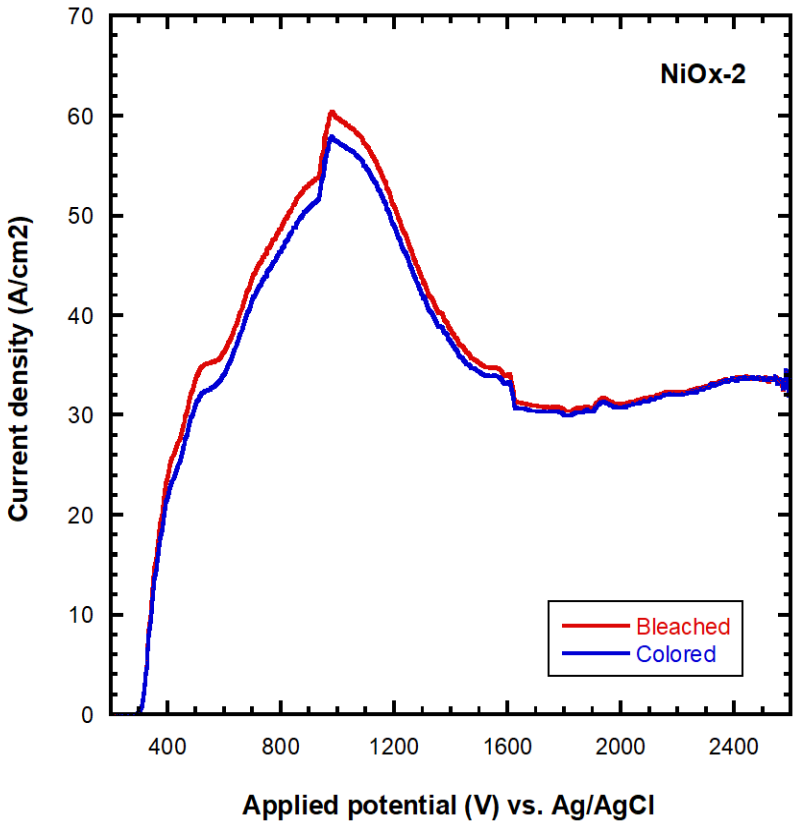

Figure 4.27. The transmittance graph of the NiO_x-2 sample in the wavelength range of 200<λ<2600

4.3.4. Indium Tin Oxide-Nickel Oxide Electrochemical Properties

The NiO_x thin film series was electrochemically cycled in 1M $LiClO_4$-PC in the potential range between -0.6 and 1.2V against Ag/AgCl for electrochemical testing. Figure 4.28. shows the voltammogram at a scanning rate of 100mV/s. Similar to WO_3 studied in this thesis, the higher the film thickness, the more current flows through the thin film, and thus the higher the anodic and cathodic peak current densities. The charge capacity is highly dependent on the sample thickness, and the addition of more Li^+ ions increase as the potential range is increased.

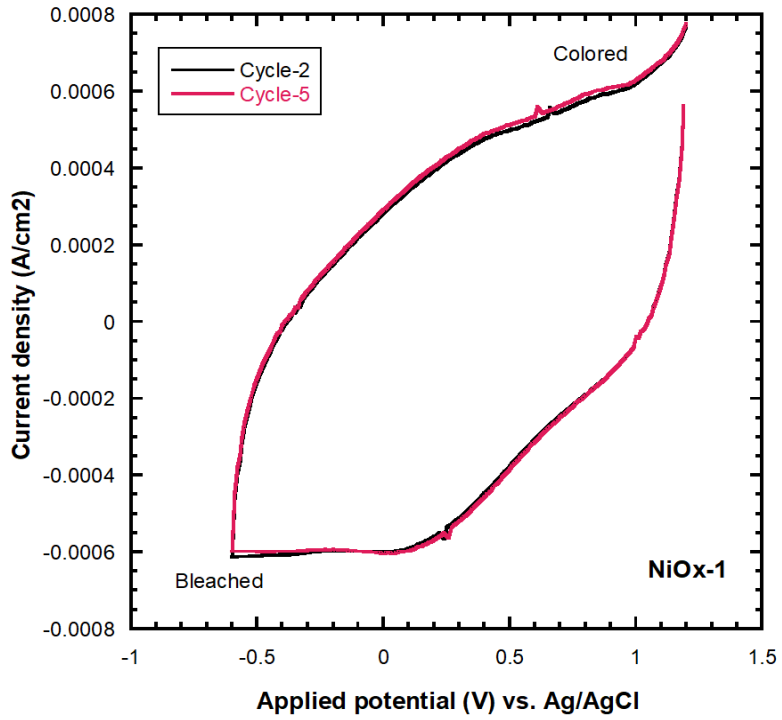

Figure 4.28. Current-voltage graph made by electrochemical CV cycling of NiO_x thin film deposited on ITO. 2 and 5 cycles for the NiO_x-1 sample

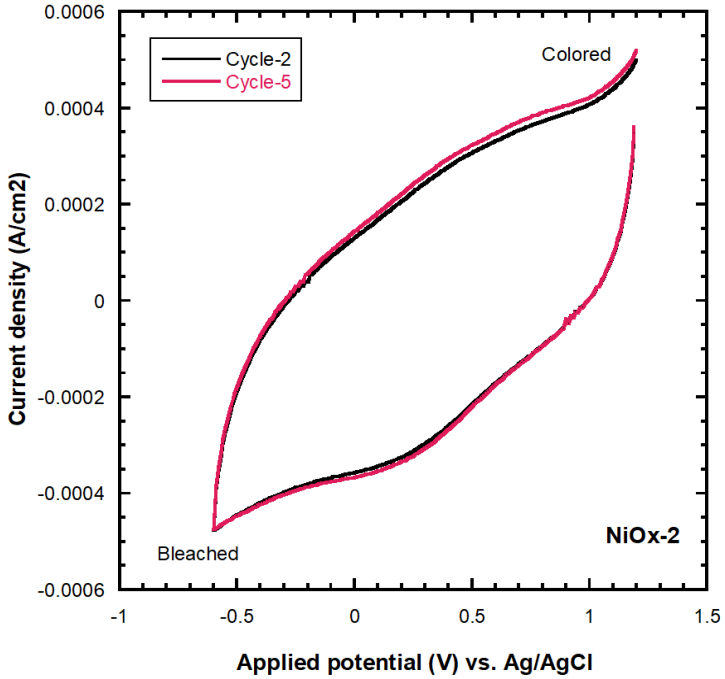

Figure 4.29. Current-voltage graph made by electrochemical CV cycling of NiO_x thin film deposited on ITO. 2 and 5 cycles for the NiO_x-2 sample

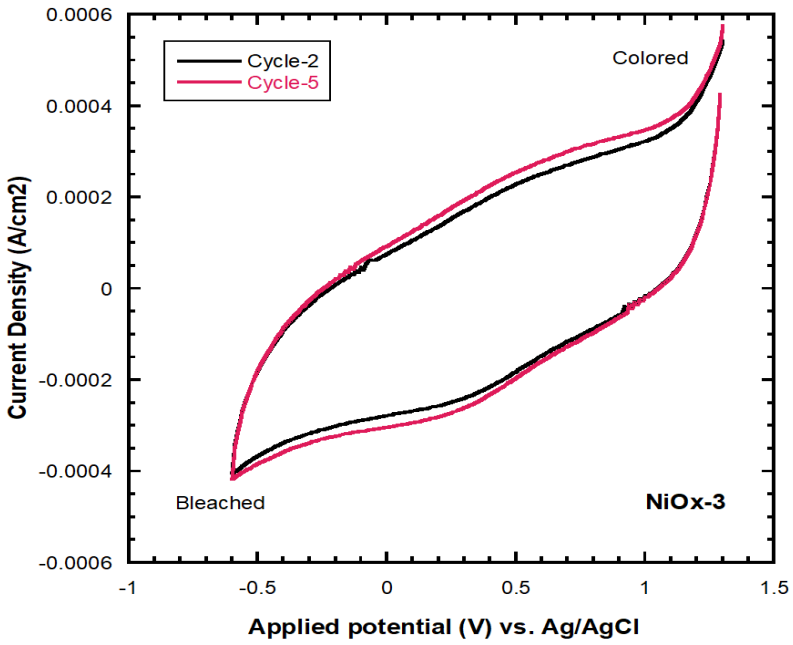

Figure 4.30. Current-voltage graph made by electrochemical CV cycling of NiO_x thin film deposited on ITO. 2 and 5 cycles for the NiO_x-3 sample

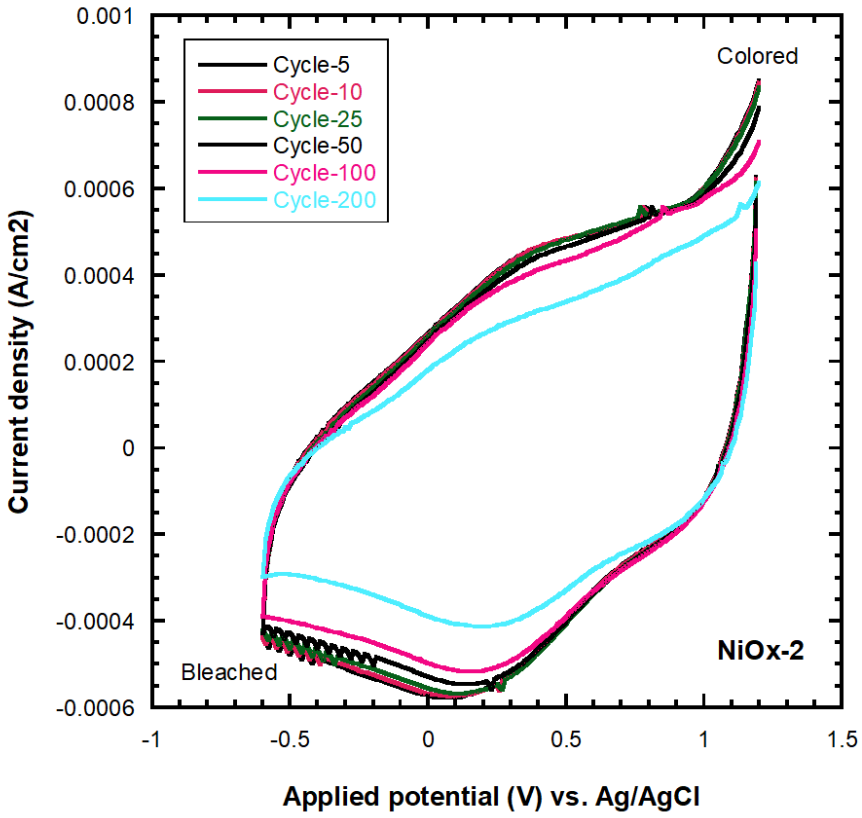

Figure 4.31. Graph of 200 cycles at -0.6 and 1.2 V and 100mV/s for the NiO_x-2 sample

NiO_x-2 sample gives the best result from the NiO_x thin film samples found here. Therefore, a CV graph of 200 cycles of this sample was created.

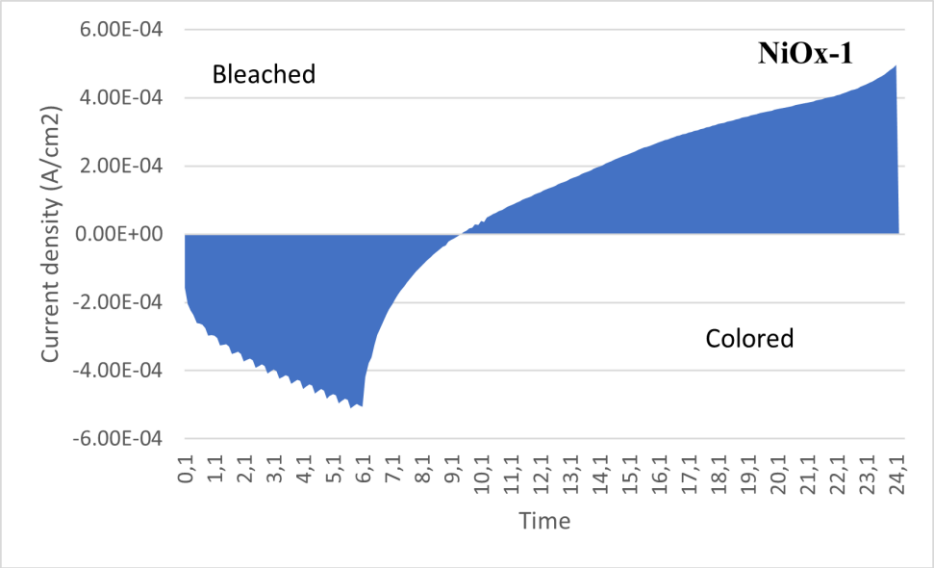

Figure 4.32. Evolution of current density basing on the 25 second CV measurement at 100 mV/s of NiO_x -1 thin film

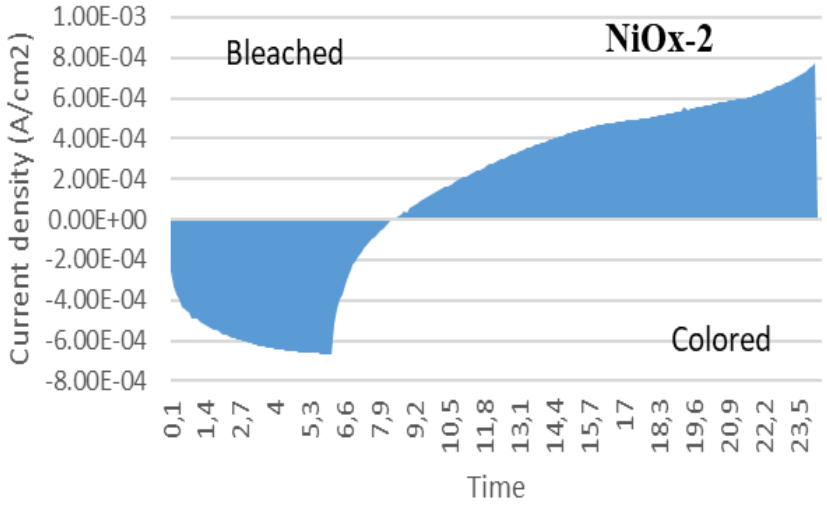

Figure 4.33. Evolution of current density basing on the 25 second CV measurement at 100 mV/s of NiO_x -2 thin film

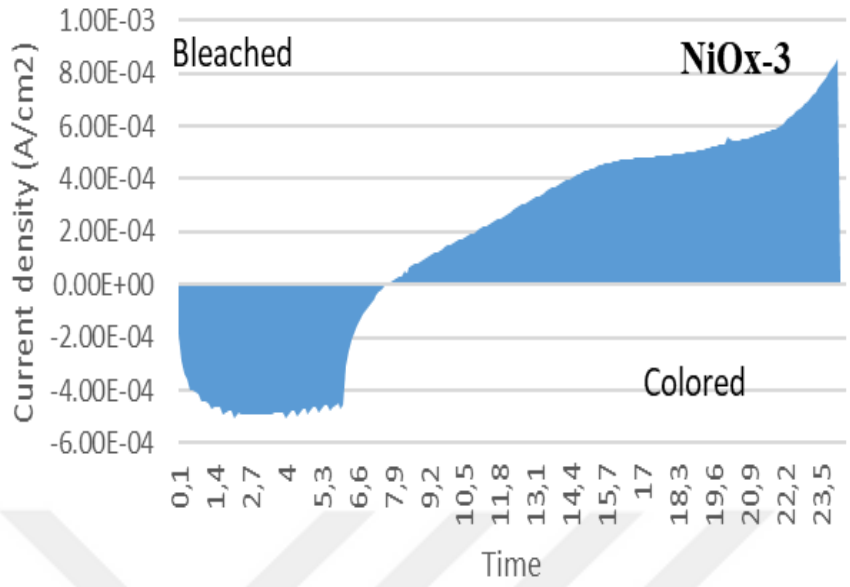

Figure 4.34. Evolution of current density basing on the 25 second CV measurement at 100 mV/s of NiO_x -3 thin film

As can be seen from the current-time graphs of glass/ITO/NiO_x coated thin films of different thicknesses, the currents drawn by the samples increase when the film thickness in NiO_x increases. This means an increase in Li^+ deposition to the samples. The best sample here is seen as glass/ITO/NiO_x-2. The bleached zone and the coloration zone are close to each other.

4.4. Tantalum Pentoxide Physical Properties

Table 4.6. The coating parameters of Ta_2O_5 samples of different thicknesses are shown. As the thickness increases, the permeability percentages of Ta_2O_5 samples increase.

Table 4.6. Thicknesses of Ta_2O_5 thin films with different deposition times on glass

Sample Number	Ar/ O_2 (sccm)	Power (W)	Deposition Time (min)	Working Pressure (hPa)	Thickness (nm)	Average Transmission (%) (λ=400-700 nm)
Ta_2O_5-1	68.5/5	50	5	$5.4x10^{-3}$	6	74.2
Ta_2O_5-2	68.5/5	50	10	$5.4x10^{-3}$	12	73.5
Ta_2O_5-3	68.5/5	50	15	$5.4x10^{-3}$	30	78.76
Ta_2O_5-4	68.5/5	50	20	$5.4x10^{-3}$	45	84.63

4.4.1. Indium Tin Oxide-Tantalum Pentoxide Physical Properties

In this part, deposition parameters of Ta_2O_5 samples grown on indium tin oxide coated thin film are included. Due to the increase in coating times, the thickness of the films increases. But the permeability percentages are increasing. Percentages of transmittance shown here are average percentages in the 400-700 nm range.

Tablo 4.7. Deposition parameters of Ta_2O_5 samples coated on glass/ITO

Sample Number	Ar/ O_2 (sccm)	Power (W)	Deposition Time (min)	Working Pressure (hPa)	Thickness (nm)	Average Transmission (%) (λ=400-700 nm)
ITO-Ta_2O_5-1	68.5/5	50	5	$5.4x10^{-3}$	225/6	77.3
ITO-Ta_2O_5-2	68.5/5	50	10	$5.4x10^{-3}$	225/12	77.6
ITO-Ta_2O_5-3	68.5/5	50	15	$5.4x10^{-3}$	225/30	78.4
ITO-Ta_2O_5-4	68.5/5	50	20	$5.4x10^{-3}$	225/45	82.6

4.4.2. Tantalum Pentoxide Optical Properties

Ta_2O_5 thin films of 4 different thickness parameters are given in Figure 4.35. The thickness map of the sample numbered Ta_2O_5-4 is shown in Figure 4.36. Here, the thickness map is determined by the photoresists we drip onto the glass surface.

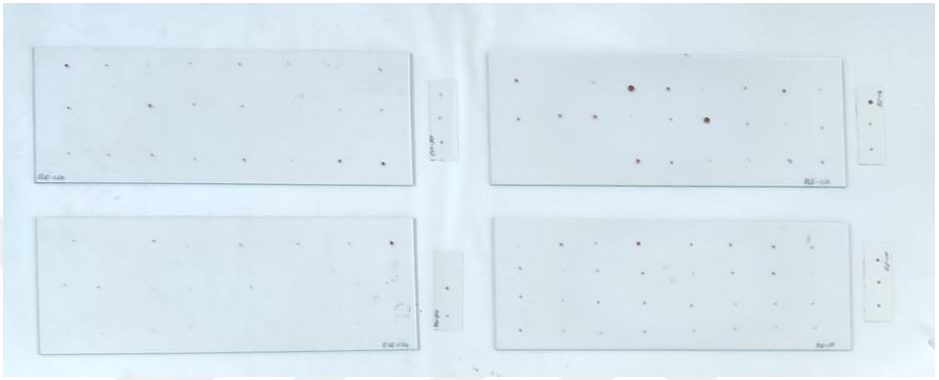

Figure 4.35. Ta_2O_5 coated glasses

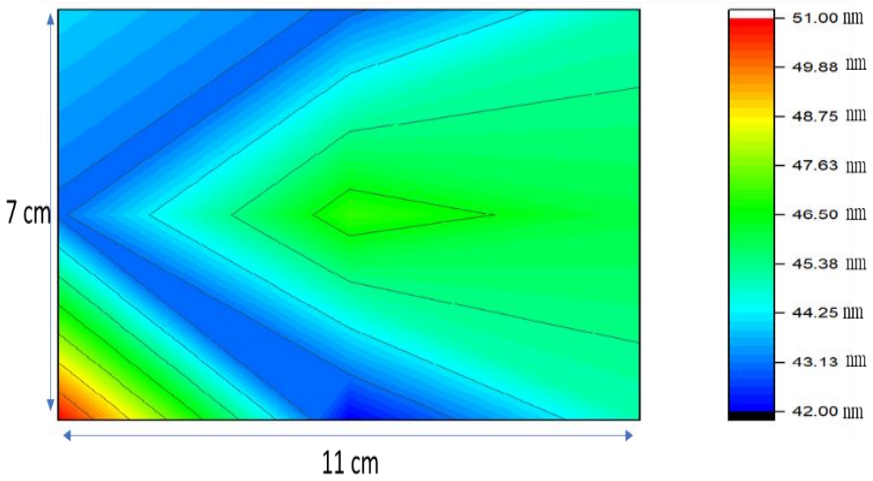

Figure 4.36. Ta_2O_5- 4 thickness mapping

The transmittance graph of Ta_2O_5 samples belonging to 4 different coating times Figure 4.37. given.

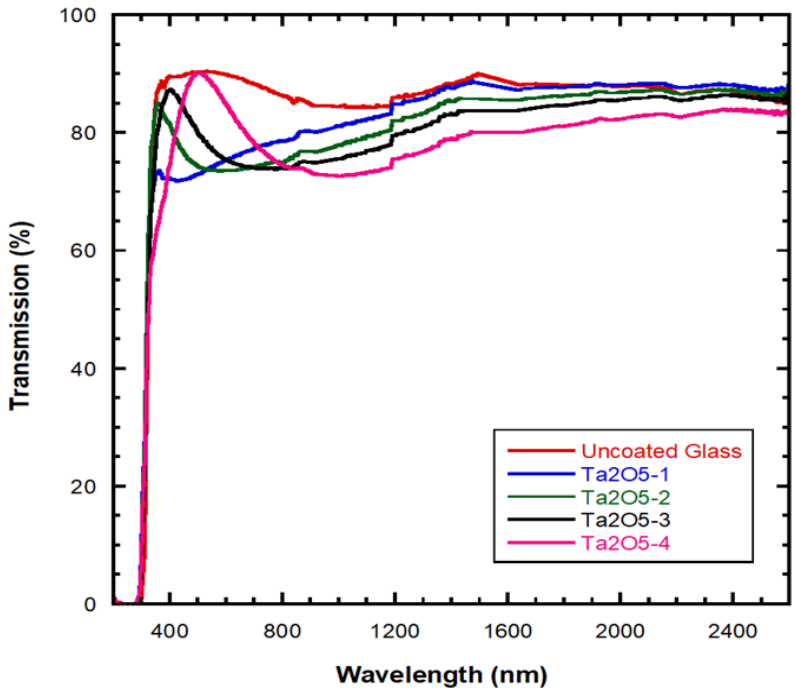

Figure 4.37. Transmittance graph of Ta_2O_5 samples

4.4.3. Indium Tin Oxide-Tantalum Pentoxide Optical Properties

Figure 4.38., shows 4 samples of Ta_2O_5 with different parameters deposition on indium tin oxide. In Figure 4.38., the permeability graphs of these samples are compared.

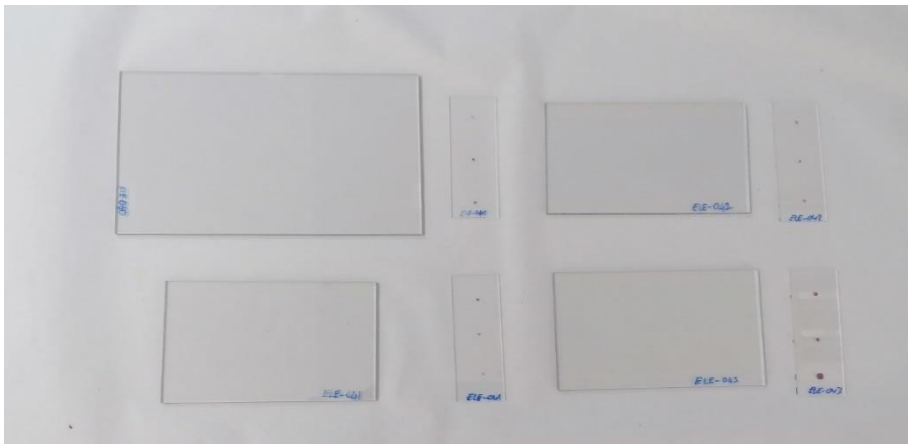

Figure 4.38. ITO-Ta_2O_5 coated glasses

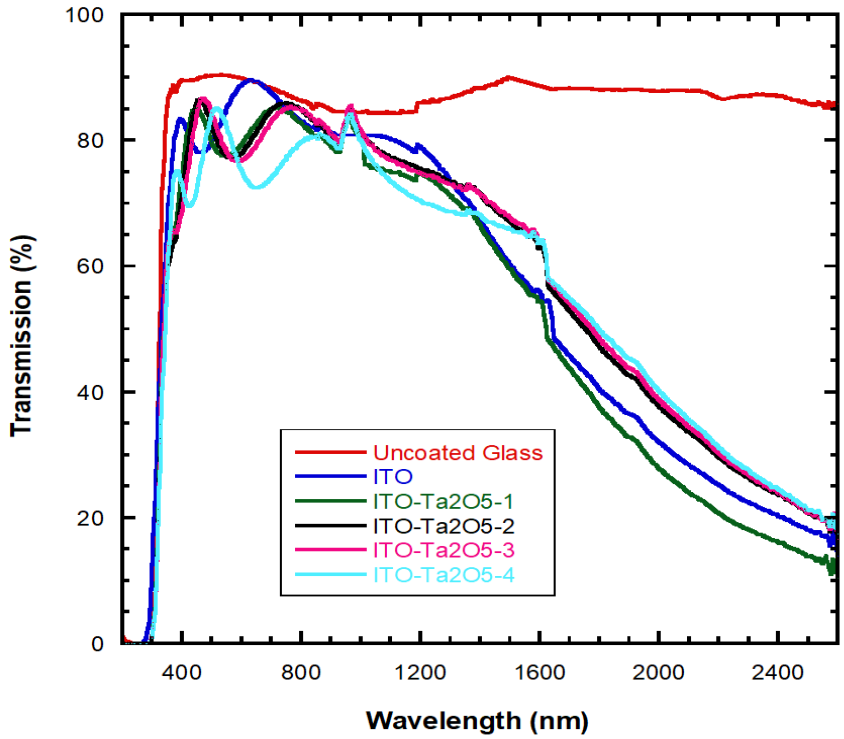

Figure 4.39. Transmittance graph of ITO-Ta_2O_5 samples

4.4.4. Indium Tin Oxide-Tantalum Pentoxide Ion Conductive Properties

The aluminium contact taken from the Ta_2O_5 sample deposition on indium tin oxide is taken as in figure 4.40. In Figure 4.41., a sample of aluminium contact is given.

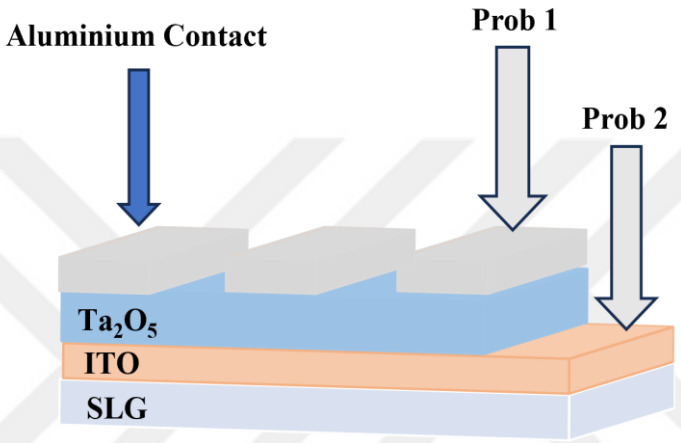

Figure 4.40. Al contact designation of glass/ITO/Ta_2O_5 coated sample

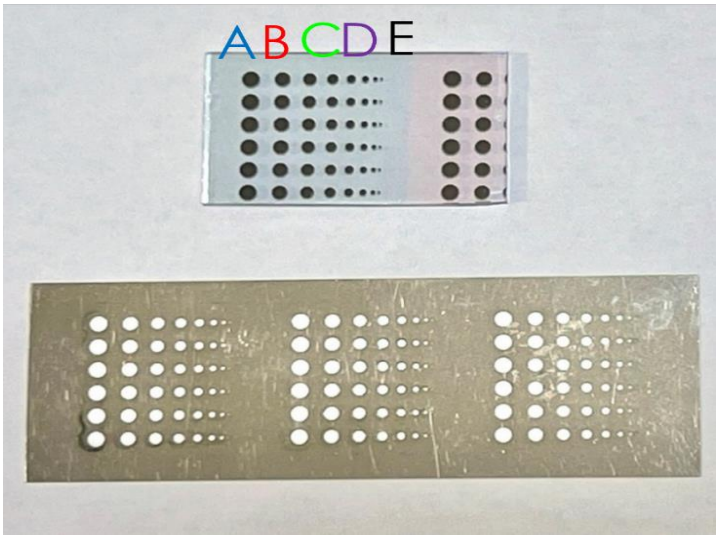

Figure 4.41. Al contact of glass/ITO/Ta_2O_5 sample

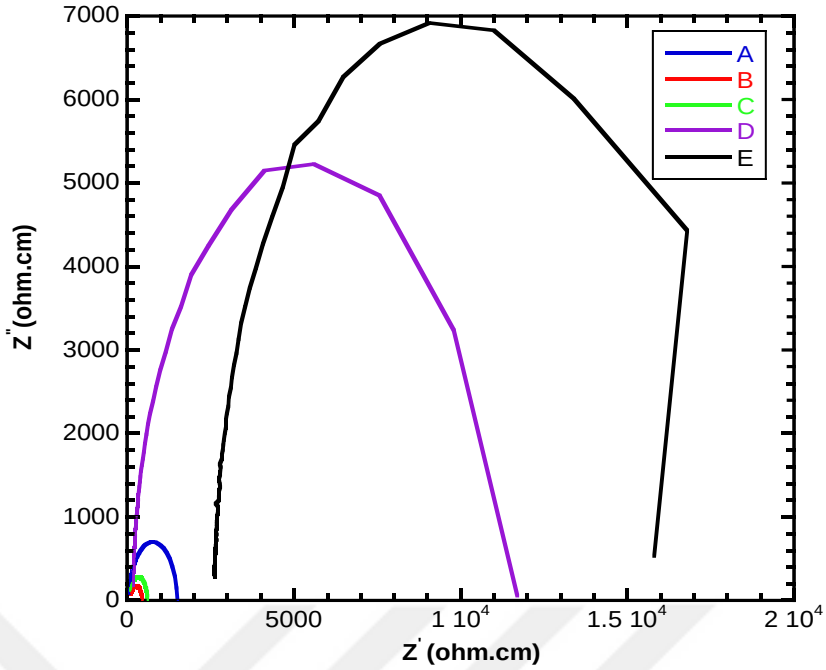

Figure 4.42. Ionic conductivity graph of glass/ITO/Ta_2O_5-2 coated sample

In Figure 4.42. the ionic conductivity graph of the aluminum contact sample is shown. It is seen here that there are different ionic conductivities in different electrode areas. The equation by which ionic conductivity is calculated is given in Equation 4.1. In this equation, d=electrolyte thickness, A=electrode area and R=electrolyte resistance. As a result of this equation, ionic conductivity was found in the range of $\sigma = 1x10^{-5}$-$7x10^{-7}$ $S.cm^{-1}$.

$$\sigma = \frac{d}{(RxA)} \tag{4.1}$$

4.5. Assembling of the ECD

Coated images of ZAZ-WO_3-Ta_2O_5-NiO_x are shown in Figure 4.43. and ITO-WO_3-Ta_2O_5-NiO_x samples are shown in Figure 4.44. Measurements of the permeability graphs of these samples were made. Using ZAZ instead of ITO provides better electrical conductivity and higher optical properties for our ECD samples.

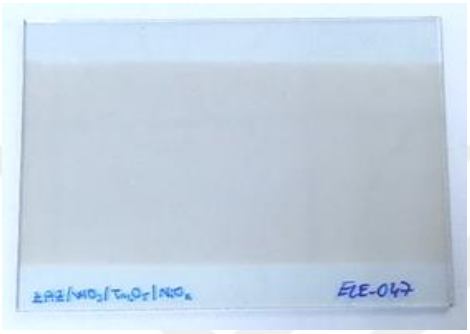

Figure 4.43. ZAZ-WO_3 -Ta_2O_5-NiO_x

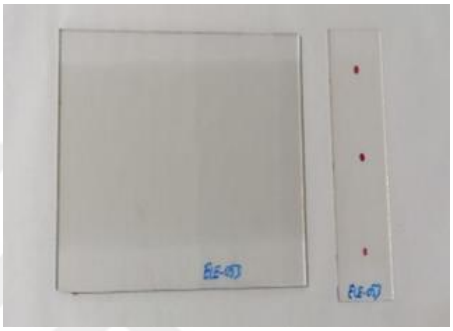

Figure 4.44. ITO-WO_3-Ta_2O_5-NiO_x

In Figure 4.45., the layers of my electrochromic device that we have created are indicated. In Figure 4.46., a comparison of the permeability graph of the electrochromic device formed by using different transparent conductivity oxides is made.

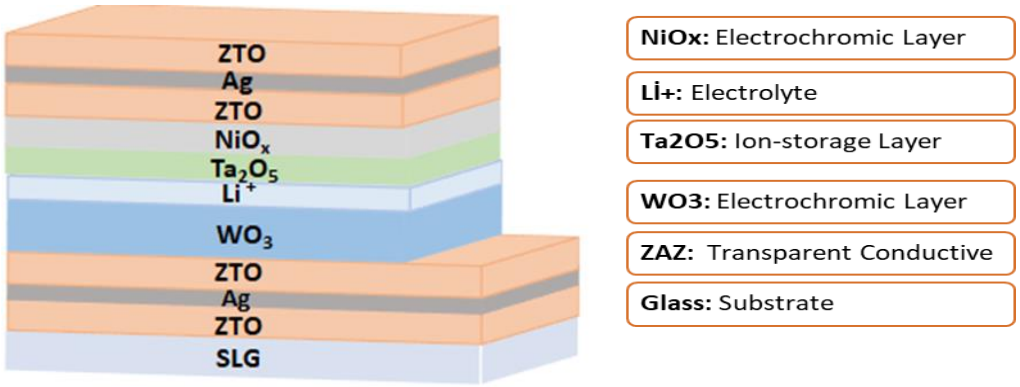

Figure 4.45. The structure of the created electrochromic device

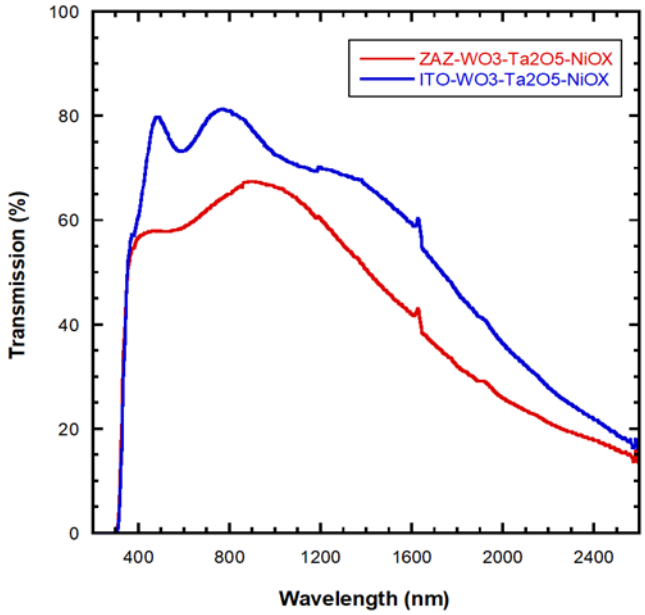

Figure 4.46. Transmittance graphs of glass/ ZAZ-WO_3 -Ta_2O_5-NiO_x and glass/ITO-WO_3-Ta_2O_5-NiO_x

CHAPTER 5

CONCLUSION

In this study, electrochromic metal oxides WO_3 and NiO_x were satisfactorily deposited with Ar/O_2 gas mixture during the coating process using DC magnetron sputtering technique. It can be deduced from XRD that WO_3 and NiO_x thin films have amorphous structure. In cyclic voltammetry, a porous structure was deduced from the color change because of the ion insertion/extraction process. A prototype electrochromic device was assembled to determine the performance of the electrochromic thin film series. The results showed good optical modulation over 250 cycles of the WO_3 sample with a thickness of about 180 nm in combination with a NiO_x sample with a thickness of 110 nm, as well as fast switching time by applying -1.0/1.2 V. Experiments also show that WO_3 thin films with higher thicknesses in combination with 110 nm thick NiO_x result in ion trapping. Due to the increase in WO_3 thin film thicknesses, a decrease in the optical properties caused by the transition from colored to transparent state and therefore a decrease in optical transmittance was observed. Depending on the Ta_2O_5 thicknesses, changes are also seen in the ionic conductivity graphs. It has been determined that the thickness of the Ta_2O_5 coated thin films used here is also important.

In general, the results obtained in this thesis are effective in the formation of WO_3 and NiO_x thin films with slow deposition rates by magnetron sputtering technique. The important part here is that the thin films grown by the magnetic sputtering method exhibit low defect. This is an important advantage in creating electrochromic devices.

REFERENCES

Abu-Yaqoub, Atheer Yousef Saleh. Electrochromic Properties of Sol-gel NiO–based films. Diss. 2012.

Ahn, Kwang-Soon, et al. "All-solid-state electrochromic device composed of WO_3 and Ni $(OH)_2$ with a Ta_2O_5 protective layer." Applied physics letters 81.21 (2002): 3930-3932.

Al-Kahlout, Amal. "Electrochromic properties and coloration mechanisms of sol-gel NiO-TiO_2 layers and devices built with them." (2006).

Aparicio, Mario, Andrei Jitianu, and Lisa C. Klein, eds. Sol-gel processing for conventional and alternative energy. Springer Science & Business Media, 2012.

Baedeker, Karl. Über die elektrische Leitfähigkeit und die thermoelektrische Kraft einiger Schwermetallverbindungen. JA Barth, 1906.

Balk, Pieter. "Dielectrics for field effect technology." Advanced Materials 7.8 (1995): 703-710.

Bamfield, Peter. Chromic phenomena: technological applications of colour chemistry. Royal Society of Chemistry, 2010.

Bessière, Aurélie, et al. "Flexible electrochromic reflectance device based on tungsten oxide for infrared emissivity control." Journal of applied physics 91.3 (2002): 1589-1594.

Chiang, H. Q., et al. "High mobility transparent thin-film transistors with amorphous zinc tin oxide channel layer." Applied Physics Letters 86.1 (2005): 013503.

Choudhary, Yogesh S., Lavanya Jothi, and Gomathi Nageswaran. "Spectroscopic Methods for Nanomaterials Characterization." (2017): 19-54.

Ding, Jingjing, et al. "Study of electrochromic characteristics in the near-infrared region of electrochromic devices based on solution-processed amorphous WO3 films." Materials Science in Semiconductor Processing 88 (2018): 73-78.

Dong, Dongmei, et al. "Lithium trapping as a degradation mechanism of the electrochromic properties of all-solid-state WO_3//NiO devices." Journal of Materials Chemistry C 6.37 (2018): 9875-9889.

Elgrishi, Noémie, et al. "A practical beginner's guide to cyclic voltammetry." Journal of chemical education 95.2 (2018): 197-206.

Forrister, B. T. (2018). Analyzing Cyclic Voltammetry at a Microdisk Electrode with Simulation. Retrieved 3 July 2018, from https://www.comsol.com/blogs/analyzingcyclic-voltammetry-at-a-microdisk-electrode-with-simulation.

Ghodsi, Farhad E., Fatma Z. Tepehan, and Galip G. Tepehan. "Optical properties of Ta_2O_5 thin films deposited using the spin coating process." Thin Solid Films 295.1-2 (1997): 11-15.

Ghorannevis, Z., E. Akbarnejad, and M. Ghoranneviss. "Structural and morphological properties of ITO thin films grown by magnetron sputtering." Journal of Theoretical and Applied Physics 9 (2015): 285-290.

Gillaspie, Dane T., Robert C. Tenent, and Anne C. Dillon. "Metal-oxide films for electrochromic applications: present technology and future directions." Journal of Materials Chemistry 20.43 (2010): 9585-9592.

Granqvist, Claes Göran, et al. "Electrochromic materials and devices for energy efficiency and human comfort in buildings: A critical review." Electrochimica Acta 259 (2018): 1170-1182.

Guo, Junji, et al. "Prominent electrochromism achieved using aluminum ion insertion/extraction in amorphous WO3 films." The Journal of Physical Chemistry C 122.33 (2018): 19037-19043.

Higashitani, Ko, Cathy E. McNamee, and Masaki Nakayama. "Formation of large-scale flexible transparent conductive films using evaporative migration characteristics of Au nanoparticles." Langmuir 27.6 (2011): 2080-2083.

Hongwei, Fan, et al. "Multi-functional Electrochromic Devices: Integration Strategies Based on Multiple and Single Devices." JOURNAL OF INORGANIC MATERIALS 36.2 (2021): 115-127.

Jang, Wei-Luen, et al. "Point defects in sputtered NiO films." Applied Physics Letters 94.6 (2009): 062103.

Jayathilake, D., and T. Nirmal Peiris. "Overview on transparent conducting oxides and state of the art of low-cost doped ZnO systems." SF J Material Chem Eng1 (1) 1004 (2018).

Jiao, Zhihui, et al. "Hydrothermally grown nanostructured WO_3 films and their electrochromic characteristics." Journal of Physics D: Applied Physics 43.28 (2010): 285501.

Jittiarporn, Phuriwat, et al. "Electrochromic properties of sol–gel prepared hybrid transition metal oxides–A short review." Journal of Science: Advanced Materials and Devices 2.3 (2017): 286-300.

Kim, Taewhan, et al. "Applications of voltammetry in lithium-ion battery research." Journal of Electrochemical Science and Technology 11.1 (2020): 14-25.

Kongsat, Pantharee, et al. "Synthesis of structure-controlled hematite nanoparticles by a surfactant-assisted hydrothermal method and property analysis." Journal of Physics and Chemistry of Solids 148 (2021): 109685.

Koseoglu, Hasan, et al. "Improvement of optical and electrical properties of ITO thin films by electro-annealing." Vacuum 120 (2015): 8-13.

Kraft, Alexander. "Electrochromism: a fascinating branch of electrochemistry." ChemTexts 5.1 (2018): 1.

Lee, K.-S., Koo, H.-J., Ham, K.-H., Ahn, W.-S., MO Calculation for the oxygen interaction with Ni24(100) Model Surface, Bulletin of the Korean Chemical Society, 16, 1995.

Li, Y., P. L. Tremblay, and T. Zhang. "Anode Catalysts and Biocatalysts for Microbial Fuel Cells." Progress and Recent Trends in Microbial Fuel Cells; Elsevier: Amsterdam, The Netherlands (2018): 143-165.

Lin, Yung-Sen, Yue-Liang Chiang, and Jhen-Yi Lai. "Effects of oxygen addition to the electrochromic properties of WO_3− z thin films sputtered on flexible PET/ITO substrates." Solid State Ionics 180.1 (2009): 99-105.

Liu, Qirong, et al. "In situ electrochromic efficiency of a nickel oxide thin film: origin of electrochemical process and electrochromic degradation." Journal of Materials Chemistry C 6.3 (2018): 646-653.

Ekmekcioglu, Merve, et al. "High transparent, low surface resistance ZTO/Ag/ZTO multilayer thin film electrodes on glass and polymer substrates." Vacuum 187 (2021): 110100.

Moorthy, Suresh Babu Krishna, ed. thin film structures in energy applications. Springer, 2015.

Nie, Yujie, et al. "Transmission-matrix Quantitative Phase Profilometry for Accurate and Fast Thickness Mapping of 2D Materials." ACS Photonics 10.4 (2023): 1084-1092.

Niklasson, Gunnar A., and Claes G. Granqvist. "Electrochromics for smart windows: thin films of tungsten oxide and nickel oxide, and devices based on these." Journal of Materials Chemistry 17.2 (2007): 127-156.

Ozer, N., and C. M. Lampert. "Electrochromic performance of sol-gel deposited WO_3–V_2O_5 films." Thin Solid Films 349.1-2 (1999): 205-211.

Pajkossy, Tamás. "Voltammetry coupled with impedance spectroscopy." Journal of Solid-State Electrochemistry 24.9 (2020): 2157-2159.

Pandurang, Ashrit. Transition metal oxide thin film based chromogenics and devices. Elsevier, 2017.

Park, Sung-Ik, et al. "A review on fabrication processes for electrochromic devices." International Journal of Precision Engineering and Manufacturing-Green Technology 3 (2016): 397-421.

Park, Sung-Ik, et al. "A review on fabrication processes for electrochromic devices." International Journal of Precision Engineering and Manufacturing-Green Technology 3 (2016): 397-421.

Patel, K. J., et al. "An investigation of the insertion of the cations H^+, Na^+, K^+ on the electrochromic properties of the thermally evaporated WO_3 thin films grown at different substrate temperatures." Materials Chemistry and Physics 124.1 (2010): 884-890.

Platt, John R. "Electrochromism, a possible change of color producible in dyes by an electric field." The Journal of Chemical Physics 34.3 (1961): 862-863.

Qiu, H., Y. F. Lu, and Z. H. Mai. "Electrochromic writing and erasing on tungsten oxide films in air by scanning tunneling microscopy." Journal of applied physics 91.1 (2002): 440-443.

Qiu, Jianhua, et al. "Effect of O_2 Concentration on the Electrochromic Properties of NiO_x Films." Journal of Nanoscience and Nanotechnology 18.7 (2018): 4814-4821.

Rai, Varun, and Chee-Seng Toh. "Electrochemical amplification strategies in DNA nanosensors." Nanoscience and Nanotechnology Letters 5.6 (2013): 613-623.

Rai, Varun, Jiajia Deng, and Chee-Seng Toh. "Electrochemical nanoporous alumina membrane-based label-free DNA biosensor for the detection of Legionella sp." Talanta 98 (2012): 112-117.

Roland, Jean-François, and Fred C. Anson. "Incorporation of redox-active cations into tungsten oxide coatings on electrodes: enhancement of coating stability and electrocatalytic activity." Journal of Electroanalytical Chemistry 336.1-2 (1992): 245-261.

Rosseinsky, David R., Paul MS Monk, and Roger J. Mortimer, eds. Electrochromic materials and devices. John Wiley & Sons, 2015.

Rubio, F., et al. "Sputtered Ta_2O_5 antireflection coatings for silicon solar cells." Thin Solid Films 90.4 (1982): 405-408.

Sauvet, K., L. Sauques, and A. Rougier. "IR electrochromic WO_3 thin films: from optimization to devices." Solar Energy Materials and Solar Cells 93.12 (2009): 2045-2049.

Schmidt, H., et al. "Indium-free bottom electrodes for inverted organic solar cells with simplified cell architectures." Applied Physics Letters 99.3 (2011): 141.

Shinriki, H., et al. "Oxidized Ta/sub-2/O/sub-5//Si/sub 3/N/sub-4/dielectric films on poly-crystalline Si for dRAMs." IEEE transactions on electron devices 36.2 (1989): 328-332.

Shinriki, Hiroshi, and Masayuki Nakata. "UV-O/sub-3/and dry-O/sub-2: Two-step-annealed chemical vapor-deposited Ta/sub-2/O/sub-5/films for storage dielectrics of 64-Mb DRAMs." IEEE Transactions on electron devices 38.3 (1991): 455-462.

Sone, Yoshitsugu, et al. "Reversible electrochromic performance of Prussian blue coated with proton conductive $Ta_2O_5 \cdot nH_2O$ film." Solid state ionics 83.1-2 (1996): 135-143.

Tajima, Kazuki, et al. "Electrochemical evaluation of Ta2O5 thin film for all-solid-state switchable mirror glass." Solid State Ionics 180.6-8 (2009): 654-658.

Tajima, Kazuki, et al. "Solid electrolyte of tantalum oxide thin film deposited by reactive DC and RF magnetron sputtering for all-solid-state switchable mirror glass." Solar energy materials and solar cells 92.2 (2008): 120-125.

TF, Baeck SH Choi KS Jaramillo. "Stucky GD McFarland EW Enhancement of photocatalytic and electrochromic properties of electrochemically fabricated mesoporous WO_3 thin films." Adv. Mater 15 (2003): 1269-1273.

Thirumalai, Jagannathan. "Introductory Chapter: The Prominence of Thin Film Science in Technological Scale." Thin Film Processes-Artifacts on Surface Phenomena and Technological Facets. IntechOpen, 2017.

Tu, Yuan-Ruang, et al. "Characterization of Reactively Rf-Sputtered Tantalum Oxide Waveguides." Optoelectronic Materials, Devices, Packaging, and Interconnects. Vol. 836. SPIE, 1987.

Tuna, Ocal, et al. "High quality ITO thin films grown by dc and RF sputtering without oxygen." Journal of Physics D: Applied Physics 43.5 (2010): 055402.

Wang, Sheng-Chang, Kuang-Yi Liu, and Jow-Lay Huang. "Tantalum oxide film prepared by reactive magnetron sputtering deposition for all-solid-state electrochromic device." Thin Solid Films 520.5 (2011): 1454-1459.

Wen, Rui-Tao, Claes G. Granqvist, and Gunnar A. Niklasson. "Eliminating degradation and uncovering ion-trapping dynamics in electrochromic WO_3 thin films." Nature materials 14.10 (2015): 996-1001.

Wu, Shih-jeh Jimmy, Boen Houng, and Bo-sen Huang. "Effect of growth and annealing temperatures on crystallization of tantalum pentoxide thin film prepared by RF magnetron sputtering method." Journal of alloys and compounds 475.1-2 (2009): 488-493.

Wu, Wei, et al. "Electrochromic metal oxides: recent progress and prospect." Advanced Electronic Materials 4.8 (2018): 1800185.

Xu, Jian Wei, Ming Hui Chua, and Kwok Wei Shah, eds. Electrochromic smart materials: fabrication and applications. Royal Society of Chemistry, 2019.

Zeng, Kaiyang, et al. "Investigation of mechanical properties of transparent conducting oxide thin films." Thin solid films 443.1-2 (2003): 60-65.

Zhang, Xiang, et al. "Preparation and performances of all-solid-state variable infrared emittance devices based on amorphous and crystalline WO_3 electrochromic thin films." Solar Energy Materials and Solar Cells 200 (2019): 109916.